From Relative to Absolute Configuration of Complex Natural Products: Interplay Between NMR, ECD, VCD, and ORD Assisted by *ab initio* Calculations

Ana G. Petrovic[a], Armando Navarro-Vázquez[b] and José Lorenzo Alonso-Gómez[b,*]

[a]*Department of Chemistry, Columbia University, 10027 New York, USA*

[b]*Departamento de Química Orgánica, Universidade de Vigo, 36310 Vigo, Spain*

Abstract: This minireview is addressed to readers with a background in basic organic chemistry and spectroscopy, but without a specific knowledge of NMR, ECD, VCD and ORD. Herein we summarize the role of quantum mechanical *ab initio* prediction of spectral properties in NMR and chiroptical spectroscopies. Illustrative examples of the application of prediction of chemical shifts and scalar couplings to the determination of chemical constitution and relative configurations of natural products are presented. Once the relative configuration is determined, the absolute configuration can be established with the help of ECD, VCD and ORD spectroscopies assisted by quantum mechanical prediction of the corresponding spectra. The scope, limitations and advantages of these chiroptical spectroscopies are presented, in order to help the reader in choosing a suitable combination of *ab initio* and spectroscopic tools when facing a particular problem.

Keywords: Relative configuration determination, absolute configuration determination, NMR, ECD, VCD, ORD, ab initio, natural products.

INTRODUCTION

Nature still surprises chemists with an astonishing variety of chemical structures. Isolation and identification of such substances takes advantage of a wide array of spectroscopic techniques, among which nuclear magnetic resonance (NMR) spectroscopy plays a distinctive role [1]. Even the large information content thereby provided, may not lead to an unambiguous establishment of the connectivity [2]. As most natural products incorporate several chiral motifs, an additional challenge is the determination of the relative configuration (RC) of constituting stereogenic centers which in turn govern the conformational properties. Furthermore, in addition to RC and conformational stereochemical features, the absolute configuration (AC) of the stereogenic centers has a profound impact on a variety of molecular properties, such as chemical reactivity and catalytic, biological, and pharmacological activities. In light of the above considerations, full stereochemical assignment of a given system is of fundamental importance in many different fields, spanning from chemical physics to biochemistry. Due to the challenge typically posed by such stereochemical analysis, the search for new and more effective methods, often based in *ab initio* quantum mechanical (QM) modeling of molecular properties, has stimulated great attention within the chemical community. The recent progress in *ab initio* methods and computer hardware makes computations in even medium size molecules (*ca*. 10^2 non-hydrogen nuclei) feasible. This has particularly helped to the fast development of chiroptical spectroscopic methods in AC determination [3], which are currently in wide use for studying the structures of chiral molecules. The most frequently used of these methods are electronic circular dichroism (ECD) [4, 5], optical rotatory dispersion (ORD), [6] and vibrational circular dichroism (VCD) [7, 8].

Optical rotation (OR) measurement at a single wavelength, oldest chiroptical method, has been widely reported by organic chemists as a physical property characteristic of any chiral compound. Although OR at a single wavelength has been used in the past for the AC assignment, nowadays optical rotation at multiple wavelengths (ORD) is considered more reliable. Additionally elucidation of AC simply based on correlations of empirical OR values for molecules with a homologous stereogenic core is strongly discouraged. The use of experimental ECD is another technique that is very useful for secondary structure elucidation of organic- and bio-molecules of wide structural diversity. While the empirical or semiclassical theoretical models used for interpretation of the experimental ECD spectra are successful in many cases, there are examples where these interpretations yielded either ambiguous or incorrect conclusions about the molecular structure. In this respect, the recent advance in *ab initio* simulations of the ECD and ORD spectra has opened much broader application opportunities for both spectroscopies. VCD as a relatively newer sibling of chiroptical methods offers additional options for molecular structure determination and its application for determining the AC also benefits for the advance in theoretical predictions. VCD is the extension of electronic CD (ECD) into the infrared (IR) region of the electromagnetic spectrum that represents an analogous form of differential absorption spectroscopy between left and right circularly polarized IR radiation by mirror-image stereoisomers.

The aim of this mini-review is to discuss the scope and interplay between NMR, ECD, VCD, and ORD, in combination with their corresponding *ab initio* QM predictions on small natural products, in order to help the reader in choosing an appropriate combination of tools when facing a particular problem by selection of recent illustrative examples (from 2006 to date).

SCOPE AND LIMITATIONS OF NMR, VCD, ECD, AND ORD

NMR is the most important and widely used method for structure determination of natural products in solution, and more recently also in solid state. Determination of connectivity through classical NMR structural analysis relies mainly on a combination of 1D and 2D experiments. Routinely, the RC of stereogenic centers is established by a combination of NOE based experiments and determination of torsion angles trough vicinal scalar couplings. Advances in probe technology and the use of inverse detected experiments allow the recording of ^{1}H and ^{13}C spectra with very small amounts of samples (< 1 mg). However, in some cases unequivocal determination of RC cannot be achieved due to structural complex-

*Address correspondence to this author at the Departamento de Química Orgánica, Universidade de Vigo, 36310 Vigo, Spain; Tel: 0034986812309; Fax: 0034986812262; E-mail: lorenzo@uvigo.es

1385-2728/10 $55.00+.00

ity. In these cases, the application of more sophisticated methods such as the use of residual dipolar couplings [9-11] or the prediction of chemical shifts and scalar couplings in a more quantitative way with the help of QM methods is desirable [12, 13].

NMR experimental data are in most cases acquired in non-chiral media and therefore the AC cannot be determined unless either the configuration of some of the centers is previously known, or the molecule is chemically derivatized with chiral auxiliaries [14]. In such approach, the assignment of AC is easily and straightforward performed by semiquantitative analysis of anisotropic effects on the ^{1}H chemical shifts, relying in previously determined conformational model. The establishment of these models, however, requires a very big effort, and confidence in the methodology can be limited by the structural similarity between the studied systems and the model. For a long time, interpretation of chiroptical properties through empirical rules has been employed for AC determination [15, 16]. However, it is very often the case where the conformational flexibility, or the large number of centers of chirality present, make these empirical rules not reliable. Fortunately, and thanks to many software and hardware developments, the chiroptical methods arise as a very powerful tool for the determination of AC as the interaction between the electromagnetic radiation and the molecules can be modeled accurately from QM first-principles.

How to choose the most appropriate chiroptical method for AC determination of a given substrate? The answer to this question lies in considering the chemical structure of the substrate along with the scope and limitations of the three methods of choice [17]:

-ORD: Depending on the intrinsic optical rotation, from 1 mg to 10 mg of sample are needed. The use of OR at several wavelengths in nonresonant region (far from electronic absorptions) is practically much simpler than the use of ECD or VCD and no presence of UV/Vis active chromophores is needed. Calculations of electronic excited states are required. Flexible molecules may not be suitable for analysis only by ORD when simulated response for different conformers give opposite sign.

-ECD: Due to high sensitivity ($\Delta A/A$ 10^{-1} to 10^{-3}), experimental measurements require only sub-µg amounts of sample. The presence of UV/Vis active chromophores is needed. For molecules with suitable chromophores, exciton coupled theory may provide a simple and straightforward approach for AC determination. It has high sensitivity, but low signal resolution. Although it is easy to measure only few bands are resolved (sometimes only one). Calculations require predictions of electronic excited states. Very flexible molecules may also cause difficulties for analysis due to presence of multiple conformers with different populations and optical contributions.

-VCD: Due to the low sensitivity ($\Delta A/A$ 10^{-3} to 10^{-5}), experimental measurements typically require at least 10 mg of sample. Nevertheless, VCD displays high signal resolution and therefore good conformational sensitivity. Numerous vibrations could serve as IR-active probes of chirality. Typically measurements are done in IR inactive solvents (CCl_4, CS_2 and $CHCl_3$), and precaution should be taken regarding solubility. The solubility challenge can be bypassed by using solvents like DMSO-d_6 or D_2O, yet the use of these polar solvents, which can also participate in hydrogen bonding, could make necessary the inclusion of solvent effects in *ab initio* calculations. Molecules with propensity for intermolecular H bonding may require additional geometry optimization of the dimers. VCD requires only calculations within the electronic ground state and it is therefore potentially easier to model in DFT computations.

Thus, based on their scopes and limitations, one of the chiroptical methods should appear as the most suitable for a given molecule. However, a cross verification with more than one method might be necessary.

CONFORMATIONAL MODELING

In molecules with conformational flexibility the observed properties are an average over all the conformers present in solution. Therefore establishing the potential energy surface (PES), that is, identifying all the conformations with zero energy gradient (stationary points) and their relative energies is a necessary step. Depending on the number of rotatable bonds, this can be achieved by performing either systematic or random conformational search. Systematic search involves a manual setup of torsions associated with rotatable bonds, wile random search is typically based on Monte Carlo [18, 19] or simulated annealing [20, 21] based algorithms. Due to the associated computational cost, this step is typically performed with a suited molecular mechanics force-field for the molecule of interest. For general use MM3 force field [22, 23], and derivatives as MMFF94 [24-28] are especially popular since they are well parameterized for a large collection of systems. Other force fields families as OPLS [29-31] have also been employed. Once an initial ensemble of stationary points is obtained, further filtering is achieved by considering only the distinct conformations within a chosen energy window. Further geometry optimization of the selected pool of conformations is performed *via ab initio* methods where the choice on the level of the theory is made based on the nature of the system. In most cases this step is routinely performed using HF or DFT methods as they provide the best compromise between accuracy and computational time. Hybrid functionals, such as the well known B3LYP, in combination with common basis set (6-31G(d), 6-311G(d,p), etc) are the most popular choice. The QM geometries can then be further filtered according to their computed HF or DFT energies. Subsequently, harmonic frequencies along with vibrational normal modes are computed for the selected pool of conformers. The Gibbs free energies of the conformers are also obtained directly from the frequency calculation and the nature of the stationary points as true minima is verified by the absence of imaginary frequencies. However, molecules exhibiting very low frequencies (< 10 cm^{-1}) may incorporate free- and/or hindered-rotors, and therefore present a challenge for the determination of the PES [32]. There is no standard protocol for treating such systems as approaches are very much system dependent. Upon the characterization of the PES, relative population of the different minima (conformers) can be obtained by using Boltzmann relation according to their relative Gibbs free energies.

NMR (chemical shifts and scalar couplings) and chiroptical (transitions intensities and frequencies) observables may then be computed for each stable conformer in the PES. In a conformationally stable system a single minimum on the potential energy surface (PES) contributes significantly to its properties. Complications might arise when the systems under investigation are ''flexible'', that is, they exist in more than one stable conformation. In this case, the computed total theoretical prediction results from a sum of the responses, computed chemical shieldings and scalar couplings in the NMR case and computed spectra for chiroptical spectroscopies, of all relevant conformers, each of them weighted by its population fraction determined according to Boltzmann statistics. Note that this corresponds to fast conformational exchange regime in NMR spectroscopy, since in the slow exchange regime separated chemical shifts and couplings can be observed for each conformer. A flow-

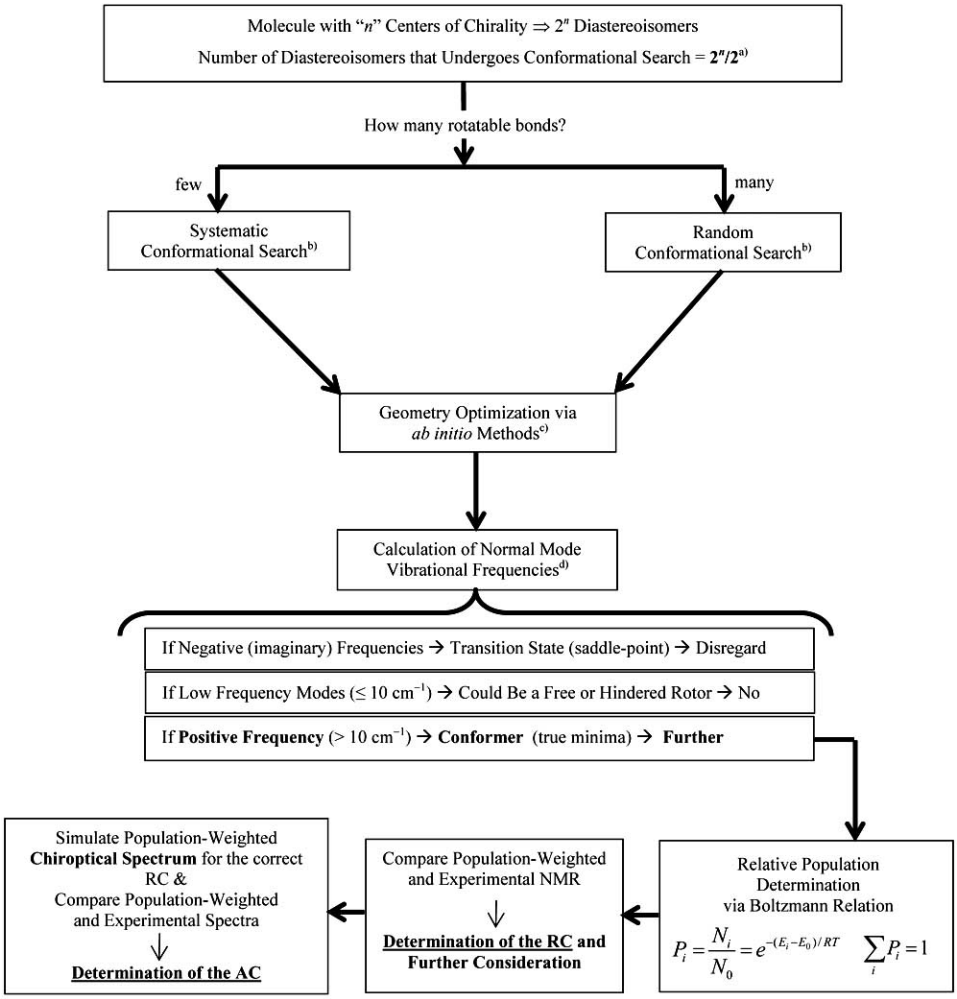

Scheme 1. Flow-chart representing for determination of RC *via* NMR to AC *via* chiroptical methods. a) Applies only to unknown RC. b) Quick geometry optimization *via* molecular mechanics (MM). c) Redundant geometries should not be considered. Only conformers within E ~ 20 kcal mol^{-1} energy window from the previous MM geometry optimization are considered. d) Only conformers within E ~ 3 kcal mol^{-1} energy window are considered.

chart representing the path from determination of RC *via* NMR to AC *via* chiroptical methods is provided in Scheme **1**. Although some standard cutoff values for frequencies and energies are displayed, please note that these may change on case-to-case basis.

In the following we will present illustrative examples of RC and AC determination assisted by QM *ab initio* computations for each of the mentioned techniques, as well some fundaments and recommendations on the QM methodologies, from the recent literature.

1. NMR

Chemists have collected a vast knowledge about the correlation of main NMR observables in liquid state high-resolution NMR, chemical shifts and scalar couplings, and chemical structure. The influence of different functional groups on the observed chemical shift is in a very approximate way additive and is possible to estimate chemical shifts by using approximate addition rules which have been often cast in a software form [33-35]. More computationally efficient approaches, currently implemented in many commercial software packages, are the so-called hierarchical organization of spherical environments (HOSE) [34, 36] or the use of neural networks [37, 38]. However, the distinction between very similar species as diastereoisomers or computations on exotic species, where there is no previous knowledge or is at least scarce, could make heuristic approaches unreliable. A similar situation is faced for the prediction of scalar couplings where a plethora of empirical Karplus-like equations [39, 40] exist not only for proton-proton $^3J_{HCCH}$ couplings but also for couplings involving heteronuclei. Some of these equations, as for instance the well-known Haasnoot-Altona equation,[41] incorporate structural corrections for the electronegativity of substituents [42], yet problems related to the similarity between the studied system and the set of data used to parameterize the equations may limit their accuracy. In these situations the *ab initio* quantum mechanical computation of shielding tensors [43] and scalar couplings [43-45] can be attractive as they are not a priory biased towards a specific set of molecules. There already exists abundant evidence about the applicability of NMR QM computations to the structural determination of natural products [46, 47, 13]. Most of the applications resort to computation of ^{13}C spectra not only due to the larger spectral window as compared to ^1H spectra, but also to smaller sensitivity of ^{13}C chemical shifts towards solvent effects and the simpler extraction of chemical shifts from ^{13}C decoupled spectra.

Chemical shielding, is a tensorial magnitude, but in solution NMR only the isotropic part of the corresponding bidimensional tensor (Eq. 1) is manifested, as the anisotropic part vanishes due to the overall molecular tumbling. The isotropic shielding σ_{iso}, is obtained from the trace of the tensor (Eq. 2) and subsequently is related to the chemical shift δ by taking an appropriate reference (Eq. 3). Although there are several methodologies to perform this kind of computations, by far the most used approach is the gauge independent atomic orbital (GIAO) [48-50], method. Other approaches, such as CSGT [48, 51], give basically identical results in the basis set limit, yet the former presents faster convergence with basis set size and it is therefore in most cases the method of choice [48].

$$\hat{\sigma} = \begin{pmatrix} \sigma_{xx}\sigma_{xy}\sigma_{xz} \\ \sigma_{yx}\sigma_{yy}\sigma_{yz} \\ \sigma_{zx}\sigma_{zy}\sigma_{zz} \end{pmatrix} \quad \text{Eq. 1}$$

$$\sigma_{iso} = \frac{1}{3}\left(\sigma_{xx} + \sigma_{yy} + \sigma_{zz}\right) \quad \text{Eq. 2}$$

$$\delta = \frac{\sigma_{iso}^{ref} - \sigma_{iso}}{1 - \sigma_{iso}^{ref}} \approx \sigma_{iso}^{ref} - \sigma_{iso} \quad \text{Eq. 3}$$

Meaningful computation of chemical shielding tensors requires the use of high-level computational methodologies [52] and a proper treatment of electron correlation, either with post-HF methods from MP2 to very expensive coupled-cluster methodologies or DFT based methodologies. Application of chemical shielding tensor computation to common organic chemistry structural problems, mainly resorts to DFT based methodologies [12, 13, 47] as post-HF methodologies become computationally prohibitive for medium size organic molecules as most natural products. Although the "true" functional should have an explicit dependence on the magnetic current *j*, [53] the error introduced by not taking into account this factor is considered a minor issue [54]. It is a known fact that non hybrid generalized gradient functionals (GGA) provide better results than their hybrid counterparts, i.e, functionals which incorporate a fraction of the exact Hartree-Fock exchange, when their performance is considered for several different nuclei. This difference is nonetheless smaller if only ^{1}H and ^{13}C shifts are taken into account and specialized hybrid functionals for ^{1}H and ^{13}C shieldings have been proposed [55]. Note however, that non-hybrid GGA's are computationally cheaper than the hybrid ones, as explicit computation of exact exchange is avoided. Tozer's GGA KT1 and KT2 functionals [56, 57] provided good absolute shielding constants over different nuclei, performing better than B3LYP or PBE0 functionals [57]. Very good performance was obtained also for the GGAs OPBE [58] and OPW91 [52] functionals, even surpassing MP2 in many cases. Truhlar has shown that the new generation of meta-GGA functionals, which depends on the kinetic energy density as their M06-L functional [59] or the VS98 (VSXC) [60] also provide excellent results.

The use of *ab initio* scalar couplings have been more scarcely used than chemical shieldings, as in many cases their comparison with experimental values may require the analysis of second order coupled spectra. The scalar coupling involves interaction between the nuclear magnetic momenta as well with those from the electrons. The non-relativistic Ramsey's formulation [61] splits these interactions into four terms, the Fermi-Contact term (FC), the spin-dipolar term (SD) and the paramagnetic (PSO) and diamagnetic (DSO) spin-orbit terms. As the FC term is the most important contribution in ^{1}H–^{1}H and ^{1}H–^{13}C couplings they can be reasonably computed using only this term, at a moderate computational cost. However, several popular computer packages can straightforwardly compute all contributions, and most software packages report values computed with the four contributions.

$$J = J_{FC} + J_{SD} + J_{DSO} + J_{PSO}$$

Besides an adequate functional, a proper basis set should be chosen. Basis sets for NMR computations requires a good description of both valence and core electronic density [62]. However, most popular basis sets, as Pople's split-valence sets, are valence oriented and therefore not well suited for computation of NMR properties. Recently, Jensen has published several basis sets of different size specially suited for DFT chemical shielding [63] and scalar coupling [64] computations. The dependence of computation performance for scalar couplings on the basis set has been thoroughly studied by Frisch and coworkers [65]. They proposed the use of uncontracted basis sets with added tight *s* functions for computation of the FC term. Using this methodology, it is possible to perform computations of acceptable accuracy, even with double–ζ quality basis sets. Jensen has also noted that if the other terms are not negligible adding tight *p*, *d* and *f* functions can be also necessary [64]. It is worth to note however that application of *ab initio* methodologies to structural determination problems was performed in most cases using very standard approaches as common hybrid-GGAs functionals (B3LYP, etc) and split-valence basis sets of medium size as 6-311+G(d,p) or 6-311+G(2df,2p). As meta-GGA's are providing significant improvement on many problems associated with current functionals [66], further evaluation of their performance in the computation of magnetic properties is highly desirable.

Since chemical shifts are measured in solution, typically $CDCl_3$, D_2O, DMSO-d_6 or other solvents, solvation effects certainly have an effect on the observed shifts. The simplest way to take into account solvation in the computation of chemical shifts is to use implicit solvation models as the polarized continuum (PCM) family [67], and GIAO computations in combination with PCM solvation have been implemented in popular QM packages. The importance of solvation inclusion may become important in molecules of significant polar character. Thus, in the prediction of chemical shifts of push-pull enaminone GIAO-PCM performed better than the corresponding gas phase computations [68]. Also, much better agreement between experimental and computed ^{13}C and ^{15}N chemical shifts was obtained for several charged heteroaromatic systems when PCM solvation was included in GIAO/B3LYP/6-31G(d,p)//RHF/6-31G(d) computations (property calculation//geometry optimization) [69]. In an elegant manner, Bagno has quantified the role of explicit solvation solvent in the prediction of chemical shifts by running Car-Parrinello computations in the α-D-glucose-water system. PCM-GIAO ^{13}C shifts were computed on molecular dynamics snapshots with and without explicit water molecules. No significant effect was observed when water molecules were included in the computation and authors concluded that continuum models should be of enough accuracy in the computation of ^{13}C shifts [70].

As the chemical shift observable is related to the computed chemical shielding tensor by choosing a suitable reference, the isotropic shielding of the reference can be obtained by computation of the chemical shielding tensor for the reference compound, in most of the cases tetramethylsilane (TMS). In this way the chemical shift is obtained by the approximate equation:

$$\delta \approx \sigma_{calc}^{ref} - \sigma_{calc}$$

However, this introduces a problem because the studied molecule and the reference could not be described equivalently and hence a bias might be introduced for prediction regarding carbons of different hybridization. A way to circumvent this problem is to use of a double reference. Sarotti *et al.* recently proposed [71], the use of a double reference, methanol for sp^3 carbons and benzene for sp and sp^2 carbons respectively. This procedure has also been employed in halogen-substitued obtusallenes [72] as spin-orbit corrections [73] to the chemical shielding tensor may be important for heavy atom substituted carbons. Alternatively, the computation of a chemical shielding tensor for reference compound can be avoided if a linear relationship [74, 75] is established between the chemical shielding tensor and the chemical shift. For instance, Alkorta and coworkers established the following relationship at the GIAO//B3LYP/6-311+G(p,d) level for the ^{13}C chemical shifts [76] using a linear regression procedure.

$$\delta^{13}C = (175 \pm 0.2) - (0.963 \pm 0.0003)\sigma^{13}C$$

A fundamental question is how to evaluate the fit between the computed and experimental shifts. For this purpose, the more direct parameter is after performing regression analysis report the correlation coefficient r^2, as deviations can be negative or positive the mean absolute error MAE is commonly also reported.

$$\delta_{calc} = a + b\delta_{\exp t}$$

$$MAE = \frac{\sum^{N} \left| \delta_{calc} - \delta_{\exp t} \right|}{N}$$

Using the correlation coefficients *a* and *b* it is possible to correct the MAE for systematic bias through the CMAE parameter [77, 78]:

$$CMAE = \frac{\sum^{N} \left| \delta_{corr} - \delta_{\exp t} \right|}{N}, \text{ where } \delta_{corr} = (\delta_{calc} - a)/b$$

In many cases the structural problem is the differentiation between two proposed structures, as for instance, a pair of diastereoisomers. As in this scenario many deficiencies of the model computation can be removed by not comparing the computed and experimental shifts but the difference between chosen pairs of signals *a* and *b*, a new index ws proposed [77], called CP3 and defined as:

$$CP3 = \frac{\sum f_3(\Delta_{\exp}, \Delta_{calc})}{\sum \Delta^2_{\exp}}, \text{ where}$$

$$f_3(\Delta_{\exp}, \Delta_{calc}) = \begin{cases} \Delta^3_{\exp} / \Delta_{calc} \; if \Delta_{\exp} / \Delta_{calc} \geq 1 \\ \Delta^3_{\exp} \Delta_{calc} \quad \text{otherwise} \end{cases}$$

$$\Delta_{\exp} = \delta^{a}_{calc} - \delta^{b}_{calc}$$

$$\Delta_{\exp} = \delta^{a}_{\exp} - \delta^{b}_{\exp}$$

NMR in the Chemical Constitution Determination

A paradigmatic example of the value of *ab initio* chemical shifts computations is the revision of the structure of hexacyclinol, a highly oxygenated complex molecule, isolated in 2002 from *Panus rudis* [79]. The originally proposed endoperoxide structure **1a** was claimed to be synthesized later [80]. However ^{13}C GIAO computations led Rychnovsky [81] to propose **1b** as a more viable structure. The total synthesis and X-ray structure from Porco and coworkers [82] sentenced the dispute towards **1b**. Bagno *et al.* extended the analysis with computation of ^{1}H chemical shifts and scalar couplings, with again a much better fit for **1b** model [83].

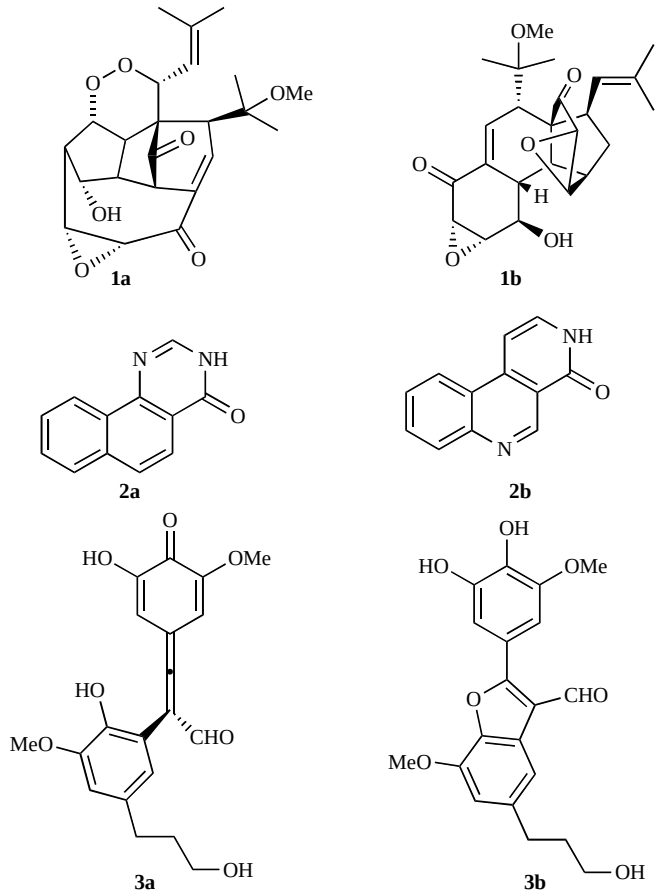

Fig. (1). Proposed (left) and revised (right) structures of hexacyclinol (**1**), samoquasine A (**2**) and *Brosimum* isolate (mururin C) (**3**).

QM computation of chemical shifts may be extremely valuable in highly aromatic molecules, as shown in the revision of structure of Samoquasine A **2b**, where standard NMR correlations may give ambiguous results [84]. They may also be a very good test for the presence of unusual functional groups. Thus, the observed deviation (> 90 ppm) between computed GIAO//B3LYP and experimental chemical shift of sp allenic carbon in **3a**, an isolate from *Brosimum acutifolium*, lead the authors to conclude that this product was in fact the already known mururin C **3b** [85]. A good example of combination of GIAO//B3LYP QM computations with standard NMR techniques was provided by Sun and coworkers in the structural determination of nortriterpenoids in combination with standard NMR methodologies [86].

NMR in RC Determination of Conformationally Stable Compounds

As a demanding test Bifulco and coworkers [87] used GIAO mPW1PW91/6-31G(d,p)//mPW1PW91/6-31G(d) computations to determine the configuration of palau'amine. The computed chemical shifts, agreed much better with a trans-fused structure and a beta orientation of the chlorine atom. Köck and coworkers arrived to the same conclusion based in NOE experiments [88]. This RC hast just been proved by total synthesis of racemic palau'amine [89].

In the same paper the authors computed the $^{3}J_{HH}$ scalar coupling between the H-C10-C11-H protons of the kedarmicin (**5**) five membered ring. The computed mPW91PW91 values clearly supported a *cis* disposition of the substituents.

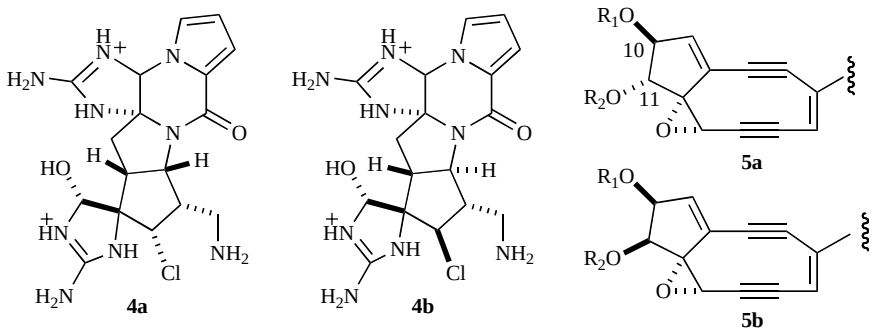

Fig. (2). Proposed (**4a**) and revised structure (**4b**) of palau'amine. Proposed (**5a**) and revised (**5b**) structure of kedarmicin.

Chemical shifts computation have also been employed for the assignment of diasterotopic groups. Thus, both DFT and MP2 GIAO computations are able to predict the right assignment of the camphene (**6**), diastereotopic *exo* and *endo* methyl groups independently determined using NOE experiments. The difference between the chemical shifts of both methyl groups was well reproduced by the GIAO computations and compared very well to heuristic HOSE computations [90]. OPBE/6-311+G(d,p)//B3LYP/6-311+G(d,p) computations were employed to quantify the shielding effect over the different conformations of phenylmenthol (**7**) as an independent control in residual dipolar couplings conformational-configurational analysis [91]. The proximity of unsaturated moieties may affect diastereotopic groups in very different way. Anisotropy effects arising from alkene and carbonyl groups, quantified at the RHF/6-311+G(d,p), were employed for assignment of diastereotopic methylene groups of longifolene and related molecules [92].

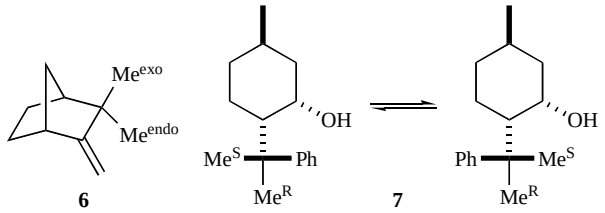

Fig. (3). Assignment of diastereotopic groups in camphene **6** and phenylmenthol **7**.

NMR in RC Determination of Conformationally Flexible Compounds

In the fast exchange regime, the NMR observables, obtained as averaged magnitudes, can be used for the determination of absolute configuration in case the AC of a pendant moiety is already known. For example, ^{1}H NMR shifts were used to determine the configuration of a highly flexible tropane derivatives **8a** and **8b** due to the large anisotropic effects of the phenyl moiety [93]. However, the interpretation of the ^{13}C shifts was ambiguous and could not differentiate between the two diastereoisomers. A similar situation was observed by Hoye and coworkers [94] in the analysis of diastereomeric lactams as **9**. However, ^{13}C shift computations, in combination with empirical *J* coupling analysis and Boltzmann averaging, furnished complete RC for all stereogenic centers in Artaborol A (**10**) showing the applicability of chemical shift computation to the stereochemical analysis of medium sized rings [95].

2. ORD

Optical rotation (OR) is a sensitive response of chiral molecules to polarized light, and is the earliest discovered chiroptical method, being therefore widely available. Optical rotation or circular birefringence refers to the rotation of the plane of linearly polarized light as it passes through the sample. The magnitude of this rotation is characteristic of each chiral compound and varies with the wavelength of the incident light (optical rotatory dispersion, ORD) and environmental conditions (temperature, solvent, pH, etc). This phenomenon was first observed by Arago in 1811 and by Biot in 1812 in quartz crystals, and Biot's later experiments established that the same rotation could be observed in solutions of camphor and turpentine [16]. Biot also introduced the modern definition of "specific rotatory power" or "specific rotation" of a solution, $[\alpha]=100\alpha/lc$, where α is the measured optical rotation in degrees, l is the optical path length in decimeters and c is grams of optically active substance in 100 ml of solution. In some instances, molar rotation $[\Phi]=[\alpha]\ M/100$ is reported, where M is the molecular weight of the optically active substance. In synthetic laboratories, specific rotation is being used for determining the enantiomeric purity of optically active samples. For a long time $[\alpha]_D$ (D stands for sodium D line at 589 nm) has also been used to determine the AC by empirical correlation or rules in a very straightforward and simple way, nonetheless as mentioned above, when many centers of chirality are

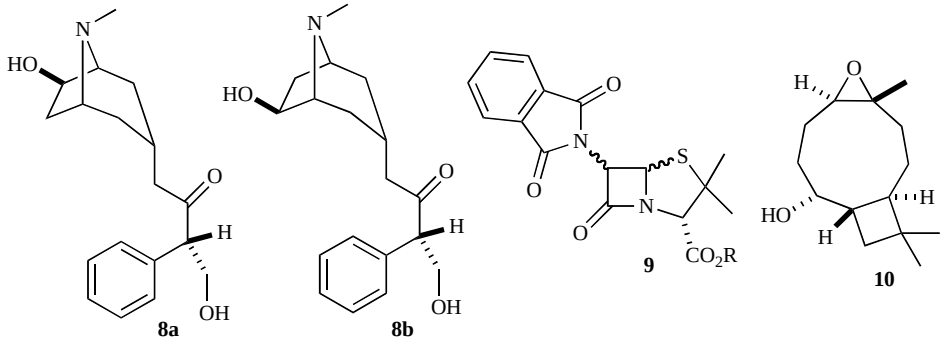

Fig. (4). Determination of relative configuration in tropanes **8**, lactame derivatives **9** and artaborol **10**.

present in the molecule, and/or the system displays high conformational flexibility, the empirical rules may not be reliable any more [96]. This status has changed dramatically in the last years, thanks to advances in quantum mechanical methods and in ever-changing computer technology, therefore producing a kind of renascence of the OR. The influence of solute-solute interactions can be avoided at infinite dilution. To achieve this, one measures the specific rotation as a function of finite concentration and extrapolates the data to zero concentration. The limiting value of specific rotation at zero concentration is referred to as the "intrinsic rotation." For a quantitative evaluation, these intrinsic rotations are the ones that are to be compared with theoretical predictions of isolated molecules [97]. One of the biggest advantages of ORD is the simplicity of measuring; one can just dissolve 1 to 10 mg of the sample in 1 mL of solvent and easily insert it into the cell to measure the optical rotation in less than a minute.

Different levels of quantum mechanical theories, including Hartree–Fock (HF) [98-101], DFT [102-106] and coupled cluster (CC) [107-109], have been developed and implemented for optical rotation predictions that are now becoming available to calculate the specific rotation for a given structure at different levels of complexity. As a consequence of these development OR has became a convenient and reliable diagnostic tool for determining the AC. If the wavelength at which the OR calculated happens to be at the resonant region (near to the wavelength of an electronic transition), theoretical prediction of OR cannot be considered reliable without additional considerations [110]. Therefore, most of the reported quantum mechanical ORD studies in the literature have relied on a nonresonant region.

The theoretical specific rotation (in units of deg.cc.g^{-1}.dm^{-1}) is obtained as:

$$[\alpha(\lambda)] = \frac{0.915\times10^{44}}{M}\sum_{k}\frac{\lambda_{ns}^2}{\lambda^2-\lambda_{ns}^2}R_{sn}$$

This equation represents the sum-over-states (SOS) expression for the nonresonant region, where R_{sn} is the rotational strength of transition n and M is the molar mass [111-115]. An alternate approach to predict ORD is to convert the ECD spectra to ORD spectra using the Kramers–Kronig (KK) transformation:

$$[\chi(\lambda_i)] = \frac{2}{\pi}\int_0^{\infty}[\theta(\lambda)]\left(\frac{\lambda}{\lambda_i^2-\lambda^2}\right)d\lambda$$

To use the KK transform method, a theoretical ECD spectrum is required, which can be simulated from the predicted rotational strengths by assuming some band profile for each ECD band. The sum in above equations extends over an infinite number of electronic transitions. This is a serious limitation with these methods because it is not known a priori where the summation can be truncated, or when the convergence can be achieved. However, the infinite summation can be avoided using linear response theory [116]. Therefore the prediction of ORD can be performed in three different ways:

– From rotational strengths using the SOS expressions.

– From the simulated ECD spectra using the KK transform.

– ECD and ORD are simultaneously obtained using the linear response method.

Generally, for quantitatively accurate results, the linear response method should be preferred over converting ECD into ORD using the SOS or KK transform expressions. On the other hand, calculations of optical rotation at a single wavelength should be discouraged since the lack in accuracy for the calculated electronic transitions could drive to errors. Very often, calculated electronic transitions appear [117-119] at lower (for Hartree–Fock methods) or higher (for B3LYP functional) wavelengths, relative to the experimentally observed electronic-transition wavelengths. For systems with multiple electronic transitions, the optical rotation sign may be of different sign at different λ, so that the calculated OR could be of different sign if the wavelength is not properly corrected (Fig. **5**) [120].

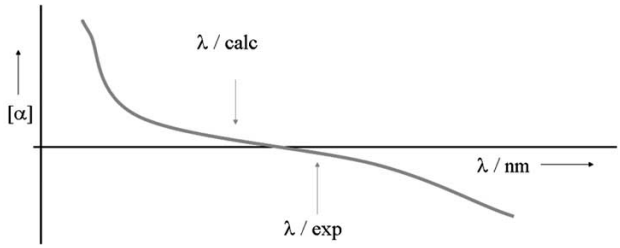

Fig. (5). Representation of optical rotation at different wavelengths.

The wavelength correction discussed for single OR calculation is not a serious issue for ORD since the general trend of the ORD experimental and calculated curves are predicted, rather than just relying on the comparison of the OR value at a single wavelength. The most frequently used level of theory for ORD predictions is B3LYP/6-31G(d), although it has been recently discussed that this is not adequate for some highly flexible molecules, as shown in the example below [121].

ORD in AC Determination of Conformationally Stable Compounds

In the case of a conformationally stable compound only one minimum on the potential energy surface (PES) considerably contributes to the total specific rotation. As an example, calculation of the ORD for the spiroiminodihydantoin nucleobases were performed on the amino and imino forms of the nucleobase Sp (*R*)-**11** and (*S*)-**11** enantiomers (Fig. **6**) geometry-optimized at the B3LYP/6-31G(d) level [122, 123].

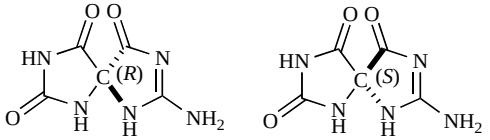

Fig. (6). Structure of (*R*) and (*S*) enantiomers of the Spiroiminodihydantoin nucleobase **11**.

The specific optical rotations were calculated using *ab initio* time dependent DFT [105, 124-127] and Gauge-Invariant Atomic Orbital (GIAO) [124, 127, 128] methods utilizing the B3LYP/6-311++G(2d,2p) basis set. The B3LYP hybrid functional is widely used in ORD computations [122, 123]. The 6-311++G(2d,2p) basis set [129-133] contains diffuse functions, which have been shown to significantly reduce basis set errors in the calculated ORD values [105]. However, calculations of the sodium D-line specific rotations of conformationally rigid molecules *via* B3LYP and other more advanced functionals, do not substantially differ in the abilities to reproduce liquid-phase experimental results [134]. Therefore, solvent and vibrational effects were not taken into account on the computed ORD values shown in Fig. (**7**).

While there are some differences in the absolute values of computed and measured specific rotation data for both enantiomers, a similar trend in the ORD experimental and simulated curves was found. It is suggested that in general differences between experi-

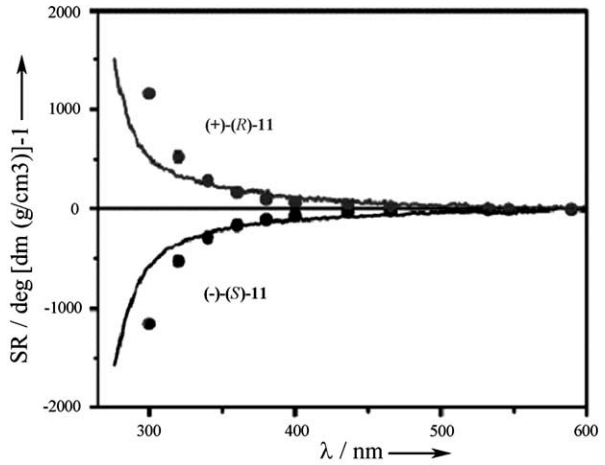

Fig. (7). Theoretical and experimental ORD of (–)-(*S*)-**11** and (+)-(*R*)-**11**. SR stands for specific rotation [α].

mental and calculated ORD are inherent to the computational methods used [117], and/or to the neglect of the solvent effects. The signs of the experimentally measured and computed ORD values indicate that Sp1 has (–)-(*S*) absolute configuration, while Sp2 has (+)-(*R*) absolute configuration for the amino tautomer. The computed ORD values shown in Fig. (**7**) were obtained for the amino tautomeric forms. However, **11** might partially exist also in the imino form, the tautomer with the exocyclic amino group being usually favored over the imino tautomer in a variety of heterocyclic ring systems [135]. On the basis of the QM geometry optimization calculations, the amino form is lower in energy by only 1 kcal/mol than the imino form [136]. Consequently, the contributions of the imino form to the specific rotation cannot be neglected a priori. The authors therefore calculated the specific rotation of the Sp imino form as well. The results show that the ORD values of the imino forms do not differ significantly from those of the amino forms, and thus, ORD cannot distinguish between the two tautomers [137]. The AC of these compounds was later reconfirmed by ECD calculations [138].

ORD in Conformationally Flexible Compounds

For conformationally flexible compounds, two examples are presented in order to show the scope and limitation of ORD for this category of systems. Namely, whenever a compound with more than one conformer contributing relevantly to the ORD, two extreme cases are possible. When the plots of the calculated ORDs for all the conformers have similar trends, for instance all positive, or when some of the conformers exhibit ORD calculated plots with opposite signs.

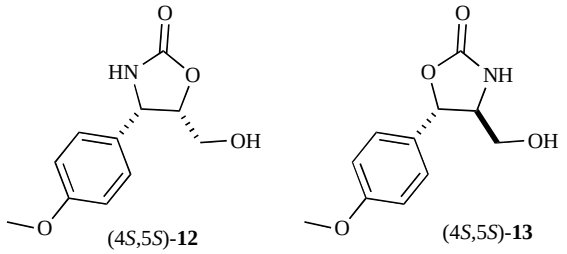

Fig. (8). Structures of (+)-(4*S*,5*S*)-*cis*-cytoxazone ((+)-(4*S*,5*S*)-**12**) and (–)-(4*S*,5*S*)-*trans*-isocytoxazone ((4*S*,5*S*)-**13**).

Ab initio calculations of the optical rotatory power of the natural cytokine [139] modulator (+)-(4*S*,5*S*)-*cis*-cytoxazone ((+)-(4*S*,5*S*)-**12**) and (–)-(4*S*,5*S*)-*trans*-isocytoxazone ((–)-(4*S*,5*S*)-**13**) (Fig. **8**), have been performed at four different wavelengths (589, 546, 435, and 405 nm) by DFT [139]. Conformational search of the *cis* derivative (+)-(4*S*,5*S*)-**12** uncovered the presence of ten conformers within 1.5 kcal mol^{-1} after geometry optimization at the B3LYP/6-31G(d) level of theory (Fig. **9**).

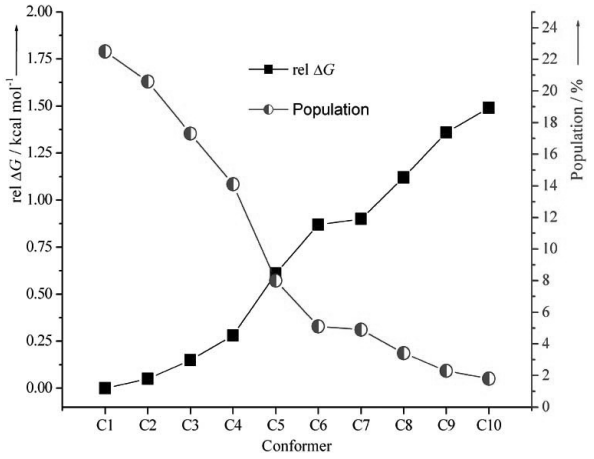

Fig. (9). Theoretical conformational distribution of (+)-(4*S*,5*S*)-*cis*-cytoxazone.

Typically errors up to 1 kcal mol^{-1} can be obtained in the determination of relative energies by many *ab initio* calculations. Nonetheless, the ORD plot for all the ten conformers was calculated (Fig. **10**). As it is shown, all the conformers have positive values for the ORD. This fact leaves no room for a possible wrong assignment of the AC due to errors in the characterization of the PES.

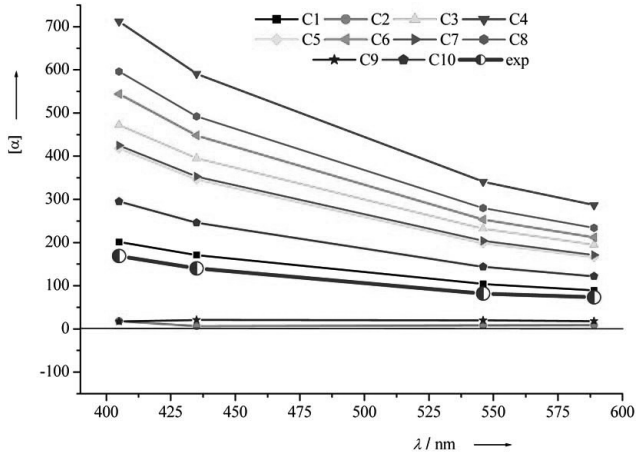

Fig. (10). Theoretical ORD plots for the different conformers of (+)-(4*S*,5*S*)-12.

On the other hand, the *trans* isomer (–)-(4*S*,5*S*)-**13** was subjected to conformational search affording also conformers within 2 kcal mol^{-1} (Fig. **11**) but on this case affording ORD signatures with opposite sign for some of the conformers (Fig. **12**).

Recently, the AC assignment of the *trans* derivative **13** has been corrected after its enantioselective synthesis. The earlier incorrect assigned was a consequence of an error in the determination on the conformational distribution. The use of a larger basis set and the consideration of solvation effects in the PES determination and

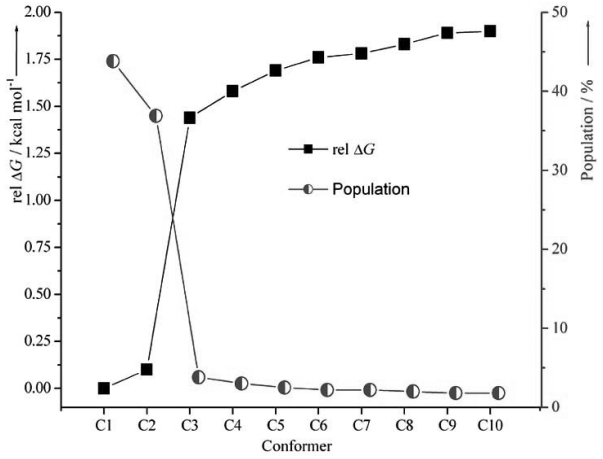

Fig. (11). Theoretical conformational distribution of (–)-(4*S*,5*S*)-*trans*-isocytoxazone 13.

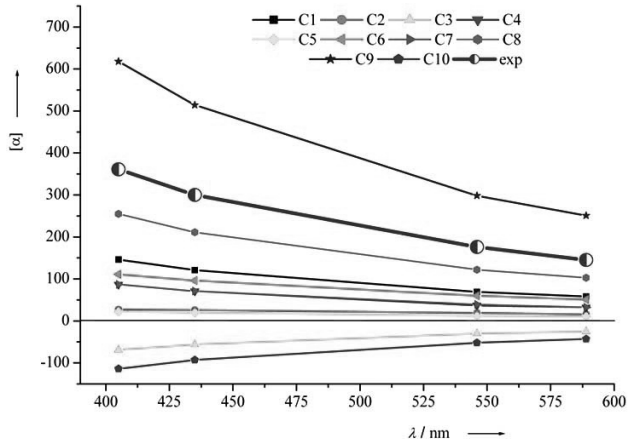

Fig. (12). Theoretical ORD plots for the different conformers of (–)-(4*S*,5*S*)-*trans*-isocytoxazone 13.

ORD simulations led in this case to the right assignment. The lesson that should be taken from this example is that if the ORD responses for the different conformers of a flexible molecule, have opposite sign, the use of other chiroptical techniques like VCD and/or ECD are highly recommended in the quest for a reliable AC assignment.

3. ELECTRONIC CIRCULAR DICHROISM (ECD)

Among the three chiroptical techniques addressed in this mini-review, ECD has been the most widely applied [4, 15, 140] over the years for structure elucidation of a diverse pool of chiral molecules. The initial application of this method has relied on semiempirical correlation rules (octant rule, exciton chirality method, etc.), yet such approaches are somewhat limited in scope due to a need for structural prerequisites. For example, to apply the exciton chirality method, the chiral molecule must contain at least two UV/Vis chromophores in order to exhibit an interpretable bisignate ECD couplet [4, 140]. Although when applicable, semiempirical rules provide a simple and very useful approach for assigning the AC, their precondition requirements can be hampering especially when elucidating the structure of novel natural products. Even the wide application of the exiton chirality method can be problematic for molecules where the electronic transitions of the two chromophores which elicit the diagnostic couplet are not well separated from the transitions of other moieties in the molecule. Since *ab initio* predictions of ECD are only conditioned by the size of the system, relying on these simulations has further extended the applicability of this popular and widely available method. A consideration of experimental and theoretical ECD allows for reliable stereochemical elucidation, regardless of the nature of the chromophores within the molecule or the presence of conformational degrees of freedom.

From an experimental standpoint, ECD measures the differential response of a chiral molecule to the modulation of UV/Vis radiation between right and left circularly polarized states. The differential absorption is commonly expressed as a differential molar absorptivity $\Delta\varepsilon$ (in $L \cdot mol^{-1} \cdot cm^{-1}$), assuming the Beer's law ($\Delta\varepsilon = \Delta A/l \cdot c$, where l stands for pathlength and c for molar concentration). The minuscule amount of sample, on the magnitude-order of a μg, represents a significant advantage of ECD over the other two chiroptical methods presented herein. From a theoretical standpoint, ECD response stems from both linear and circular oscillation of charge during electronic transitions from the ground to excited states, elicited by the absorption of the UV/Vis radiation. The linear charge oscillation is accounted for *via* electric and circular charge oscillation *via* magnetic dipole moments, as mathematically featured in the following expression:

$$R_k = \mathrm{Im}\left[\left\langle \Psi_0 \middle| \hat{\mu} \middle| \Psi_k \right\rangle \bullet \left\langle \Psi_k \middle| \hat{m} \middle| \Psi_0 \right\rangle\right]$$

Here, the so called velocity rotational strength (R in esu^2cm^2) represents the QM equivalent to the ECD intensity, $\hat{\mu}$ and $\hat{m}$ are electric and magnetic transition moment operators, respectively, while ψ_0 and ψ_k stand for ground and excited electronic state wavefunctions. In order to make theoretical spectra comparable to the experimental, the predicted value of R can be converted to a change in molar absorptivity, $\Delta\varepsilon$, *via* the following relation:

$$\Delta\varepsilon(\nu) = \frac{R_i \nu_i}{2.296 \times 10^{-39} \sqrt{\pi}\sigma} \exp\left[-\left(\frac{\nu - \nu_i}{\sigma}\right)^2\right]$$

where σ is a bandwith (mid-height width) in eV, while are frequencies ν in cm^{-1} ($\nu = 1/\lambda$, where λ is the wavelength in cm) [141]. The sign of the theoretical ECD response (R) depends on the relative orientation of the two transition moment vectors (μ and m). Considering that R is a signed quantity, it should be calculated as accurately as possible to avoid cancellation of near transitions. Methods that have been used to provide a trustworthy ECD are time dependent HF (TDHF), TDDFT, and coupled cluster (CC). The TDDFT, nevertheless, has been considered to provide the best balance between accuracy and computational cost, hence being the most frequently used method of choice. On the other hand, in the case of extensively π conjugated systems, TDHF is preferred over DT-DFT since the later method overestimates the extent of conjugation. Reliable TDDFT-based ECD predictions can be obtained using B3LYP functional and moderate to large basis sets (6-31G(d), 6-311+G(2d,2p), aug-cc-pVTZ, etc.) depending on the system. To obtain a more optimal correlation with the experimental trace, some case-studies demand variation in the choice of hybrid functionals (BPW91, BHLYP) [142]. Occasionally, a hybrid method TDDFT/MRCI (where MR stands for multi-reference and CI for configuration-interaction) [143], which takes account of the static electron correlation, yet at a high computational expense, has been applied to provide even more reliable ECD predictions.

In practice, predictions of at least 10 excited states are necessary to simulate a ECD spectrum over the typically measured range (200-800 nm). Both lorentzian and gaussian bandshapes have been utilized for simulating the theoretical ECD trace, yet the gaussian bandshape

with σ ≈ 0.2-0.4 eV is a more common choice. Additionally, it should not be neglected that the theoretical ECD prediction is accompanied by the calculation of the UV/Vis absorption. The value of molar absorptivity ε can be obtained from the *ab initio* output file by extracting the UV/Vis intensities given as dipole strengths (*D*) at different wavelengths and applying the below provided expression.

$$\varepsilon(\nu) = \frac{D_i \nu_i}{4 * 2.296 \times 10^{-39} \sqrt{\pi}\sigma} \exp\left[-\left(\frac{\nu - \nu_i}{\sigma}\right)^2\right]$$

It is a good practice to compare experimental and theoretical UV/Vis absorption bands in order to accesses the match between relative intensities and energies of electronic transitions. The discrete values of *R* or $\Delta\varepsilon$ can be converted into a smooth curve that resembles the experimental ECD spectrum *via* Lorenzian or, more commonly, Gaussian bandshape expressions. Nevertheless, we would like to emphasize that it is advisable to always display the bars representing the discrete *R* or $\Delta\varepsilon$ values, as the larger values of σ can sometimes conceal an existent low intensity transitions, hence potentially leading to ambiguous AC assignment. The practice of displaying intensity bars associated with each *R* value is especially crucial when ECD transitions are densely spaced and of alternating signs. The last example of the application section, demonstrates the utility of displaying the bars.

ECD for AC Determination in Conformationally Stable Compounds

Enantiomeric pairs of the cytotoxic pyrroloiminoquinone marine alkaloids discorhabdins have been isolated from *Latrunculia* species sponges collected at different locations around the coast of New Zealand [144]. The use of ECD for the AC determination is particularly attractive in the case of the discorhabdins due to their rigid, conformationally restrained structures and strong circular dichroism properties. To explore the feasibility and reliability of the method on this class of compounds, the authors undertook ECD calculations for (*S*,*S*)-**14** (Fig. **12**), the absolute configuration of which was previously defined by X-ray crystal analysis. The geometry of (*S*,*S*)-**14** was obtained from its crystal structure and optimized at the B3LYP/6-31G(d,p) level of theory, affording a single conformer. The ECD calculations in the gas phase at B3LYP/6-31G(d,p) and further in MeOH at B3LYP-SCRF/6-31G(d,p) level of theory showed no considerable differences. The calculated ECD spectra of (*S*,*S*)-**14** are in good agreement with the experimental one (Fig. **13**), thus securing the reliable AC assignment.

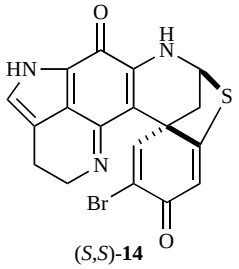

(*S*,*S*)-**14**

Fig. (12). Structure of (*S*,*S*)-**14**.

Within the category of conformational stable compounds are also those with several conformers found in the PES but where the relative energy between the global minimum and the rest of conformers is large (a few kcal mol^{-1}). In such cases, one can typically trust that the only conformation considerably contributing to the properties or the solution is the global minimum. These particular

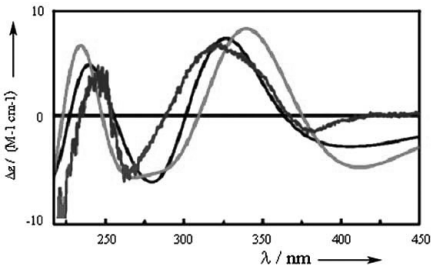

Fig. (13). Theoretical (black line calculated in gas and gray line calculated in MeOH) and experimental ECD spectrum of (*S*,*S*)-14.

scenarios demonstrate that ECD can be not only used for the AC determination but also for conformational assignment. As an example, recently it has been reported in the investigation of chiral induction from allenes into twisted butadienes, that ECD displays high sensitivity to conformational changes [145].

ECD for the AC Determination in Conformationally Flexible Compounds

The alkaloid isoschizogaline **15**, was isolated by Renner and coworkers from the east African plant *Schizozygia caffaeoides*, belonging to the Apocynaceae family, a plant used in traditional medicine in Kenya for the treatment of skin diseases. Until very recently, the AC of this natural product had not been determined.

Calculations have been carried out on (2*R*,7*R*,20*S*,21*S*)-**15**. Initial conformational analysis was carried out using Monte-Carlo searching together with the MMFF94 molecular mechanics force field. Geometry optimizations of the MMFF94 conformations obtained were then carried out using DFT, followed by calculations of their harmonic vibrational frequencies to verify their stability and to calculate Gibbs free energies. Electronic excitation energies, dipole strengths and rotational strengths of the DFT conformations have been calculated using B3LYP/aug-cc-pVDZ VDZ and ECD spectra were subsequently obtained using Gaussian band shapes.

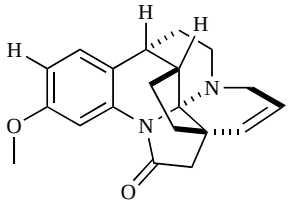

(2*R*,7*R*,20*S*,21S)-**15**

Fig. (14). Structure of (2*R*,7*R*,20*S*,21*S*)-**15**.

The outcome of the *ab initio* geometry optimization is the identification of six conformers with relative energies of 0.0, 0.9, 1.7, 2.7, 5.3 and 6.4 kcal mol^{-1}. The stability of the six conformations of (2*R*,7*R*,20*S*,21*S*)-**15** was confirmed by B3LYP/6-31G(d) harmonic vibrational frequency calculations. Thus, only three conformations are predicted to be significantly populated, with the most stable one being clearly dominant (78 %, 17% and 5 %). Further optimization of the six conformations of (2*R*,7*R*,20*S*,21*S*)-**15** at the B3LYP/TZ2P and B3PW91/TZ2P levels led to relative energies similar to the 6-31G(d) values.

The experimental ECD spectra of (2*R*,7*R*,20*S*,21*S*)-**15** as well as the calculated conformationally-averaged ECD spectra with three different bandwidths are shown in Fig. (**15**). As mentioned earlier, for cases where different transitions very close in energy display opposite rotatory strength, little changes in the bandwidth when

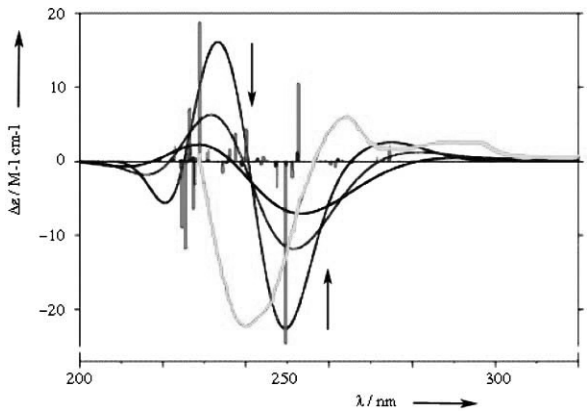

Fig. (15). Theoretical (black lines, the arrows indicate the increase in sigma 0.2, 0.3 and 0.4 when ploting the simulated data) and experimental ECD (gray line) of (2*R*,7*R*,20*S*,21*S*)-**15**. Bars depict the rotatory strength of three most stable conformers (**Ia**, **Ib**, and **IIa**).

simulating the ECD spectra can considerable change the its signature, therefore it is recommended to plot the theoretical data with several bandwidth in order to help in the comparison with the experimental one. Additionally, as discussed previously, displaying the intensity bars for the *R* values is particularly important in such cases, for example for conformer **Ia** the intensity bars emphasize the importance of correlating the ECD bands ca 270 nm in order to reliably assign the AC. The electronic excitation energies, dipolar strengths, and rotational strengths of the 20 lowest excitations of the three more stable conformers of (2*R*,7*R*,20*S*,21*S*)-**15** have been calculated at the B3LYP/aug-cc-pVDZ level of theory. The conformationally-averaged ECD spectra were obtained using Gaussian bandshapes of various σ. The comparison of calculated and experimental ECD spectra leads to the conclusion that the AC is (2*R*,7*R*,20*S*,21*S*)-(−)-**15**.

VIBRATIONAL CIRCULAR DICHROISM (VCD)

Ever since late 1990s, when instrumental advances culminated in manufacturing of the first VCD instrument [146-148] and when, coincidently, theoretical understanding of VCD matured in the implementation of the *ab initio* formulations [149-151], VCD has become an increasingly popular method of choice for elucidating the AC. Its exponential rise in usage is not only based on the fact that it represents one of the newer chiroptical approaches, but also is justified on the grounds of its advantages, including the potential for broad applicability. As a result, numerous AC elucidations [152-156] of conformationally stable and flexible natural products with multiple centers of chirality have benefited from the use of this method.

The advantageous utility of VCD is rooted in the abundance of spectral information manifested through numerous, well-resolved peaks in the mid-IR region (typically, 900-2000 cm^{-1}). Also, its high information-content stems from the fact that transitions taking place during vibrational excitations are commonly 10^2-10^3 times faster than bond rotations, hence allowing the intrinsic conformational structure of a molecule to be determined. Nevertheless, the disadvantages associated with VCD are mainly associated with its empirical implementation. Specifically, a requirement for relatively high sample quantity (~10 mg) or longer signal-collection periods ($\geq$ 1h), could preclude recording of VCD for rare or labile natural products. When obtaining the VCD spectrum, one should be mindful of solubility of a chiral molecule in typically used IR-silent solvents (CCl_4, $CHCl_3$, CH_2Cl_2, CS_2, CH_3OH), so that the combination of the concentration and pathlength can provide IR absorption ($0.2 < A < 1$) suitable for gaining a reliable VCD signal. More than one combination of concentration and pathlength might be necessary to optimize the absorption intensity in the entire detectable frequency-window. Deuterated solvents such as D_2O and DMSO-d_6 can be used when solubility in such environments is desired. The deuteration typically serves advantageously as it shifts the solvent interference bands away from those arising from the sample. For example, the biologically important aqueous media exhibits dominant O-H(D) bending modes at ~1350cm^{-1} when D_2O is used, instead of ~1550cm^{-1} when H_2O is used. Furthermore, one should be mindful that protic solvents such as H_2O and CH_3OH might affect VCD shapes by altering relative populations of various conformers through solute-solvent hydrogen bonding interactions. Such cases require incorporation of explicit or implicit (polarizable continuum model, PCM) solvent models.

Caveat should be taken, from the experimental and computational sides, when using VCD in molecules presenting hydrogen bonding. In such instances [157, 158], IR spectrum should be taken as a function of concentration within a range that encompasses the concentration employed for recording VCD. A non-linear dependence of IR bands as a function of concentration is interpreted as a diagnostic feature of intermolecular solute-solute association. If dimer formation is speculated, *ab initio* calculations should involve geometry optimization and VCD simulations of stable dimer conformations.

Ab initio VCD calculations are typically carried out at the DFT level of theory, with the hybrid B3LYP or B3PW91 functionals and 6-31G(d) or 6-311++G(2d,2p) basis sets. More sophisticated and computationally expensive augmented basis sets (aug-cc-pVTZ, aug-cc-pVQZ) have been shown to provide excellent VCD predictions, yet their use is not necessity for reliable predictions. It should be noted, nonetheless, that since VCD is a ground state chiroptical property, dependence on the exact conformation-geometries of a PES stationary points requires that *ab initio* predictions are made at exactly the same level of theory as the geometry optimization of conformers.

Similarly to ECD, the *ab initio* QM analogue for IR absorption intensity is the dipole strength (*D*), while for VCD intensity is the rotational strength (*R*). In the case of VCD, the expressions relating *D* and *R* to the corresponding experimental observables, ε and $\Delta\varepsilon$, are given as:

$$\varepsilon_0 = \frac{100}{2.303\pi\sigma} D \quad \Delta\varepsilon_0 = \frac{\nu_0}{23\pi\sigma} R$$

where σ stands for bandwidth, typically 4-6 cm^{-1}. Plotting of ε *vs.* ν as well as $\Delta\varepsilon$ *vs.* ν with Lorentzian band-shape leads to generation of a theoretical IR and VCD traces in the form that is comparable to experimental analogues.

As it is the case for the other methods addressed herein, the AC is determined from the correlation between the experimental and simulated VCD responses. Although band-to-band correlation across the entire spectrum might not be possible, VCD bands that are prominent and persist in sign among the most stable conformers can be used as diagnostic markers of the AC. When assigning the AC *via* VCD, one practical pointer is to start from the comparison of the parent IR bands. Namely, one should first identify the peak-to-peak correspondence between experimental and theoretical IR absorptions and then use these correlations to help assign the VCD correspondence. Such practice avoids that VCD correlations are

based on the match in the sign between experimental and theoretical peaks that are close in frequency positions. One should regard the match of frequency positions and relative intensities as the key criteria for scoring the degree of correspondence between experimental and theoretical traces. The sign comparison of already correlated VCD bands discloses the AC assignment. Additionally, IR absorption often serves as a secondary reference to the parent VCD in assessing the presence of predominant solution conformers. Although the case-studies chosen in the subsequent application section do not rely on the IR absorbance spectra as an aid to VCD based elucidations, we would like to encourage the present and future users of VCD to more frequently display the use of the IR absorption as an aid to the VCD analysis.

VCD for the AC Determination in Conformationally Stable Compounds

In contrast with other chiroptical techniques, for many systems the VCD signature of a particular region in the spectra can be consider as isolated from the rest. This is because vibrations associated with a particular structural fragment of the molecule do not couple with other vibrations. This feature of VCD is advantageous, and in the example provided here it demonstrates not only the potential of VCD to simultaneously unveil the AC for 2 elements of chirality (center and axial chirality), but the potential to simplify the theoretical analysis by using a truncated model systems.

The molecule under consideration herein is a dimeric natural product of (*S*)-(+)-curcuphenol **16** (Fig. **16**) and its atropisomeric dimers belong to a class of bioactive metabolites derived from a marine sponge and are characterized by the same side-chain chirality but opposite axial chirality [159].

From empirical point-of-view, the two atropisomeric dimers of curcuphenol **16** display VCD spectra with the opposite inflections in the region 1600-1425 cm^{-1} (left panel of Fig. **16**) thus pointing to important diagnostic bands solely arising from the axial chirality. On the other hand, region below ~ 1400 cm^{-1} does not distinguish the two sources of chirality, yet seems to provide an overall diastereomeric response. In order to assign the axial chirality of the dimers with already known (*S*)-(+) side-chain chirality, authors have made advantage of structural localization of certain vibrational modes by devising an idea of constructed a truncated model with a (*P*)-axial chirality.

Resorting to the truncated model has greatly simplified the theoretical analysis, since the model is conformationally stable. Specifically, the complexity due to the existence of nearly isoenergetic solution phase conformations arising from the flexible nature of the biaryl alkyl side chains has been bypassed by resorting to a methyl substitution. The truncation not only eliminates conformational flexibility, hence leading to only one stable conformer, but also permits theoretically-based visualization of VCD signals solely arising from the axial chirality.

Since atropisomeric dimers (*P*) and (*M*) contain the same side-chain chirality, taking a half of the difference in their VCD spectral signatures ((VCD_1 – VCD_2)/2) isolates the VCD features resulting solely from axial chirality. Right panel of Fig. (**17**) displays the comparison between the experimental VCD difference-spectrum and the trace of the truncated theoretical model of (*P*)-atropisomer. The striking similarities among the VCD features in the region above ~1400 cm^{-1} clearly confirm that the prominent features are solely due to the axial chirality thus allowing the AC assignment of right and left to (*P*) and (*M*) axial chirality, respectively.

Subsequent to the above example, a more recent study fully demonstrating the diagnostic power of the VCD in elucidating the AC associated of the conformationally rigid molecule with dual (center and axial) units of chirality, is provided by Polavarapu *et al.* in his investigation on a homodimeric naphthpyranone-based natural product. Nevertheless, using VCD to uncover ACs for both elements of chirality is not limited to the conformationally rigid chiral species.

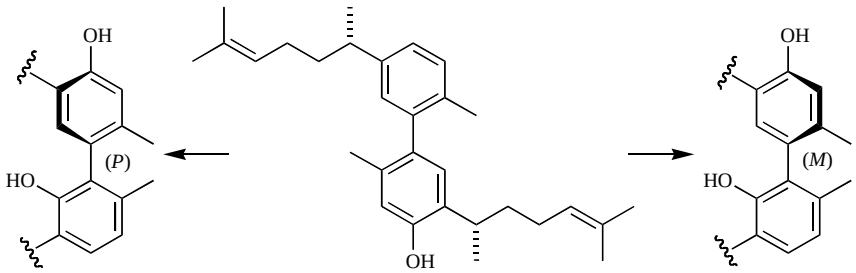

16

Fig. (16). Structure of biphenyl **16**.

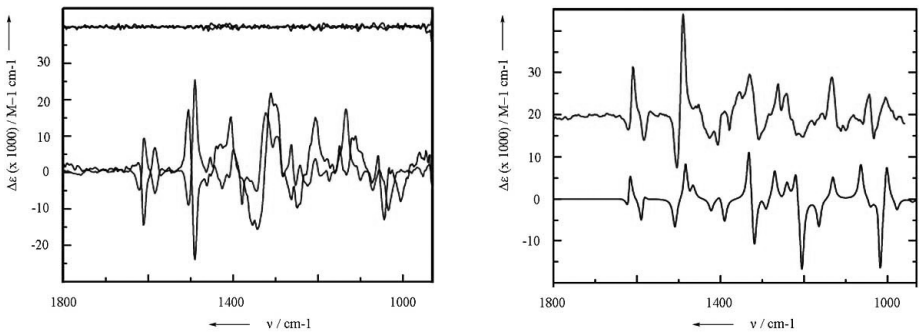

Fig. (17). Left; VCD experimental spectra of (*P*)-**16** and (*M*)-**16** and the corresponding noise. Right; theoretical spectrum of the truncated model (black line) and experimental (gray line).

VCD FOR THE AC DETERMINATION IN CONFORMATIONALLY FLEXIBLE COMPOUNDS

The overall 3D-structure of a chiral molecule, both the conformation and the configuration, is encoded in frequency position, relative intensity and sign of VCD bands. The presence of typically-observed numerous VCD bands, hence, implies a possibility of extracting structural information on multiple levels. An investigation of a natural product lippifoliane (**17**) provides compelling evidence that VCD serves as a reliable stereochemical tool for not only reliably establishing the AC, but also for verifying the relative populations of the prevailing solution-state conformers [160]. This fairly conformationally flexible chiral molecule is a secondary metabolite of a woody aromatic shrub native of Argentina, which is a traditional medicine used as a diuretic and stomachic agent.

Conformational search of **17** (Fig. **18**) was initiated with Monte Carlo (MC), based on MMFFs force-field, and subsequently subjected to DFT-based geometry re-optimization *via* B3LYP/DGDZVP level of theory. The search resulted in a pull of four stable conformers (Fig. **19**) with conformational equilibrium predominance of 92% given to conformer labeled as **a**, followed by **b**, **c**, **d** with 5%, 2%, and 0.3%, respectively.

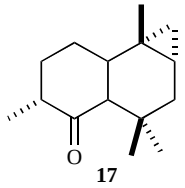

17

Fig. (18). Structure of **17**.

The theoretical VCD spectra were generated for the four conformers at the same level of theory as used for geometry optimizations. Their individual spectra along with the population-weighted theoretical spectra were compared to the experimental spectra, as displayed in Fig. (**19**). It is apparent that each conformation features a distinctive VCD signature, with especially dramatic change in intensity and phase observed for the stretching band of the C=C group at ~ 1610 cm^{-1} among the four conformers. The highly satisfactory correspondence between the population-weighted VCD spectrum and experimentally one, justifies the accurate identification of the conformer-geometries and estimation of their respective populations. As implied earlier, the overall accurate VCD response of a flexible molecule can be predicted only when the conformational minimum-energy structures and Boltzmann populations are accurately predicted. If the experimental conformations were substantially different in number, structures and relative Gibbs free energies from the predicted ones, the predicted VCD spectra would be in a poor agreement with the experiment. The quality of the agreement therefore supports the reliability of the conformation analysis, which further provides a high confidence to the AC assignment of the isolated lippifoliane **17** to the (*4R*,*9S*,*10R*)-enantiomer. A recent investigation on an even more conformationally flexible natural product, verticillane **18** (Fig. **20**) [161], which carries an important role in the biosynthesis of taxanes, provides another striking example of how revealing VCD data can be with respect to the AC and conformational distribution the most stable conformers. This chiral molecule displays a presence of six stable conformers, three with the principal population-contributions of 42%, 39%, 15% and the rest ~ 3 %. The identity and relative Gibbs free energies of these conformations have been determined by the

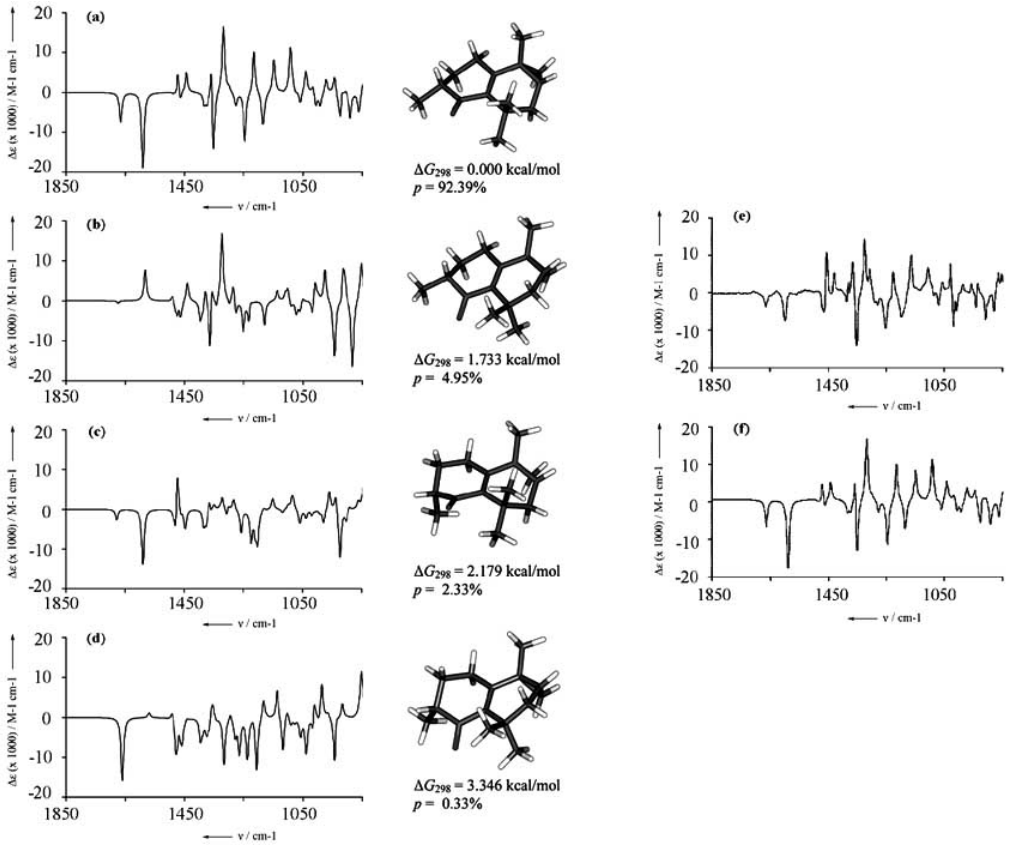

Fig. (19). Calculated spectra of conformers **a** to **d** of **17** (left). Experimental (e) and calculated (f) Boltzmann waited spectra.

same MC and DFT combined conformational search approach as in the above example. The three most stable conformers differ in the orientation of the OH-group about the commonly conformed macrocyclic carbon-framework.

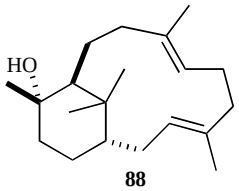

88

Fig. (20). Structure of **18**.

It can be easily noted from Fig. (**21**) that the individual VCD signatures of the three dominant conformers of **18** are considerably distinct and neither one independently results in an optimum match with the overall experimental spectra. Yet, the population-weighted VCD provides a highly satisfactory peak-to-peak correspondence between the experimental and weighted-theoretical traces. This degree of compliance exhibited in the case-study of a fairly flexible system, provides additional proof-of-concept illustrations regarding the elucidative power of VCD in validating the *ab initio* proposed relative populations of prevailing solution-state conformers.

Nevertheless, since VCD is considerably sensitive to conformations, one may encounter a case of a conformationally flexible chiral molecule with a number of low-energy conformers whose mutual presence diminishes the magnitude of many VCD bands. One such example is provided in the literature by the study of naturally occurring (+)-nyasol [162], for which correlation of only one VCD band can be used for arriving to the AC assignment. In such cases, VCD assignment must be cross-validated by resorting to ECD and/or ORD methodologies.

CONCLUSIONS AND FUTURE PROSPECTS

In this mini review, we discuss and illustrate scope, advantages and limitations of four spectroscopic methods which can be used for structure elucidation of small to moderate size chiral molecules (NMR for elucidating the RC, while ORD, ECD, and VCD for the AC). The provided examples focus on natural products, which typically present more challenging species for structure elucidation as they are often endowed with more then one center of chirality. For such, complex chiral species we recommend a two step approach, both relying on the comparison between experimental and *ab initio* data. The first step, involves the use of NMR methodologies, assisted by QM computation of chemical shifts and/or scalar couplings, in order to unambiguously establish the RC, followed by the second step, which involves the use of chiroptical method(s) in order to conclusively establish the AC. The presented applications also illustrate how tremendous progress in using *ab initio* methods along with the innovation in computer technologies has been permitting increasingly efficient predictions of spectroscopic data, which facilitate a reliable structure determination.

Given the unique advantages and empirical requirements of each chiroptical method along with simultaneous consideration of the nature of a chiral molecule, one of the three methods (VCD, ECD, & ORD) should be selected as the most suitable choice. Correspondingly, the applications provided illustrate the utility of each of the methods. Nevertheless, we would like to caution that one may encounter unforeseen challenges with the method that theoretically seems as the best choice. In such instances, one should resort to one or more chiroptical methods to insure an unambiguous AC assignment. The following complementarities among the three chiroptical methods presented strengthen the argument for their simultaneous use:

a) Vibrational transitions are numerous and better resolved than electronic transitions and so additional conformations may be identified *via* VCD that may not be apparent from ECD or ORD; on the other hand, despite the presence of a large number of vibrational transitions, many of them may not exhibit significant measurable VCD signal.

b) When different conformers of conformationally flexible molecules exhibit opposite response for a chiroptical property, the

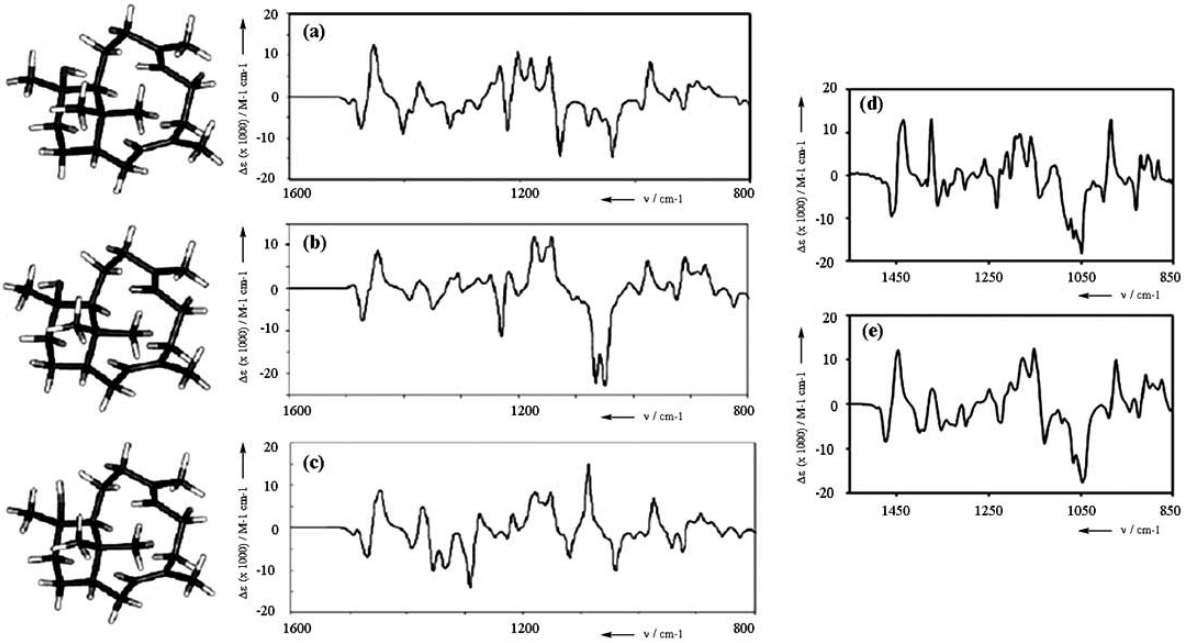

Fig. (21). Calculated spectra of the different conformers of **18** (a-c), experimental (d) and population-weighted spectra (e).

ambiguity of the AC assignment can be avoided by the use of more than one approach.

c) In the case of high density of predicted electronic transitions with alternating signs of the corresponding ECD intensities (rotational strengths), the challenge arises because spectral signature considerably changes with the choice of bandwidth; in such cases ORD can be easily applicable alternative.

ACKNOWLEDGEMENTS

We thank Prof. N. Berova for the fruitful discussions and suggestions. We acknowledge the research grants from Xunta de Galicia (PGIDIT07 PXIB 209025PR and Consellería de Educación 2009/071), Spanish MEC (CTQ2007-65310), and Universidade de Vigo. A. N. thanks the Spanish MEC for a "Ramón y Cajal" research fellowship. A. G. P. thanks University of Vigo for the travel funds.

REFERENCES

[1] Berger, S.; Sicker, D. In *Classis in Spectroscopy: Isolation and Structure Elucidation of Natural Products;* WILEY-VCH Verlag GmbH & Co. KGaA: **2009**.

[2] Nicolaou, K. C.; Snyder, S. A. Chasing molecules that were never there: Misassigned natural products and the role of chemical synthesis in modern structure elucidation. *Angew. Chem. Int. Ed.* **2005**, *44*, 1012-1044.

[3] Polavarapu, P. L. Renaissance in chiroptical spectroscopic methods for molecular structure determination. *Chem. Rec.* **2007**, *7*, 125-136.

[4] Berova, N.; Di Bari, L.; Pescitelli, G. Application of electronic circular dichroism in configurational and conformational analysis of organic compounds. *Chem. Soc. Rev.* **2007**, *36*, 914-931.

[5] Bringmann, G.; Bruhn, T.; Maksimenka, K.; Hemberger, Y. The assignment of absolute stereostructures through quantum chemical circular dichroism calculations. *Eur. J. Org. Chem.* **2009**, 2717-2727.

[6] Polavarapu, P. L. Protocols for the analysis of theoretical optical rotations. *Chirality* **2006**, *18*, 348-356.

[7] Kellenbach, E. R.; Dukor, R. K.; Nafie, L. A. Absolute configuration determination of chiral molecules without crystallisation by vibrational circular dichroism (VCD). *Spectrosc. Eur.* **2007**, *19*, 15-17.

[8] Polavarapu, P. L.; He, J. A chiral analysis using mid-IR vibrational CD spectroscopy. *Anal. Chem.* **2004**, *76*, 61A-67A.

[9] García, M. E.; Pagola, S.; Navarro-Vázquez, A.; Philips, D. D.; Gayathri, C.; Krakauer, H.; Stephens, P. W.; Nicotra, V.; Gil, R. R. Stereochemistry determination by powder X-Ray diffraction and NMR spectroscopy residual dipolar couplings. *Angew. Chem. Int. Ed.* **2009**, *48*, 5670-5674.

[10] Schuetz, A.; Murakami, T.; Takada, N.; Junker, J.; Hashimoto, M.; Griesinger, C. RDC-enhanced NMR spectroscopy in structure elucidation of sucro-neolambertellin. *Angew. Chem. Int. Ed.* **2008**, *47*, 2032-2034.

[11] Fares, C.; Hassfeld, J.; Menche, D.; Carlomagno, T. Simultaneous determination of the conformation and relative configuration of archazolide A by using nuclear Overhauser effects, J couplings, and residual dipolar couplings. *Angew. Chem. Int. Ed.* **2008**, *47*, 3722-3726.

[12] Bifulco, G.; Dambruoso, P.; Gomez-Paloma, L.; Riccio, R. Determination of relative configuration in organic compounds by NMR spectroscopy and computational methods. *Chem. Rev.* **2007**, *107*, 3744-3779.

[13] Riccio, R.; Bifulco, G.; Cimino, P.; Bassarello, C.; Gomez-Paloma, L. Stereochemical analysis of natural products. Approaches relying on the combination of NMR spectroscopy and computational methods. *Pure Appl. Chem.* **2003**, *75*, 295-308.

[14] Seco, J. M.; Quiñoá, E.; Riguera, R. The assignment of absolute configuration by NMR. *Chem. Rev.* **2004**, *104*, 17-117.

[15] Nakanishi, K.; Berova, N.; Woody, R. W. *Circular Dichroism: Principles and Applications.* WILEY-VCH, New York **1994**.

[16] Barron, L. D. In *Molecular Light Scattering and Optical Activity;* Cambridge University Press: Cambridge, **2004**.

[17] Autschbach, J. Computing chiroptical properties with first-principles theoretical methods: Background and illustrative examples *Chirality* **2009**, *21*, S116-S152.

[18] Rubinstein, R. Y.; Kroese, D. P. In *Simulation and the Monte Carlo Method;* John Wiley & Sons.: New York, **2007**, 341.

[19] Metropolis, N.; Ulam, S. The Monte Carlo method. *J. Am. Stat. Assoc.* **1949**, *44*, 335-341.

[20] Kirkpatrick, S.; Gelatt Jr., C. D.; Vecchi, M. P. Optimization by simulated annealing. *Science* **1983**, *220*, 671-680.

[21] Metropolis, N.; Rosenbluth, A. W.; Rosenbluth, M. N.; Teller, A. H.; Teller, E. Equation of state calculations by fast computing machines. *J. Chem. Phys.* **1953**, *21*, 1087-1092.

[22] Allinger, N. L.; Yuh, Y. H.; Lii, J. H. Molecular mechanics. The MM3 force field for hydrocarbons. *J. Am. Chem. Soc.* **1989**, *111*, 8551-8566.

[23] Lii, J. H.; Allinger, N. L. Molecular mechanics. The MM3 force field for hydrocarbons. 3. The van der Waals' potentials and crystal data for aliphatic and aromatic hydrocarbons. *J. Am. Chem. Soc.* **1989**, *111*, 8576-8582.

[24] Halgren, T. Merck molecular force field .1. Basis, form, scope, parameterization, and performance of MMFF94. *J. Comput. Chem.* **1996**, *17*, 490-519.

[25] Halgren, T. Merck molecular force field .2. MMFF94 van der Waals and electrostatic parameters for intermolecular interactions. *J. Comput. Chem.* **1996**, *17*, 520-552.

[26] Halgren, T. Merck molecular force field .3. Molecular geometries and vibrational frequencies for MMFF94. *J. Comput. Chem.* **1996**, *17*, 553-586.

[27] Halgren, T.; Nachbar, R. Merck molecular force field .4. Conformational energies and geometries for MMFF94. *J. Comput. Chem.* **1996**, *17*, 587-615.

[28] Halgren, T. Merck molecular force field .5. Extension of MMFF94 using experimental data, additional computational data, and empirical rules. *J. Comput. Chem.* **1996**, *17*, 616-641.

[29] Damm, W.; Frontera, A.; Tirado-Rives, J.; Jorgensen, W. L. OPLS All-Atom force field for carbohydrates. *J. Comp. Chem.* **1997**, *18*, 1955-1970.

[30] Jorgensen, W. L.; Maxwell, D. S.; Tirado-Rives, J. Development and testing of the OPLS All-Atom force field on conformational energetics and properties of organic liquids. *J. Am. Chem. Soc.* **1996**, *118*, 11225-11236.

[31] Jorgensen, W. L.; Tirado-Rives, J. The OPLS [optimized potentials for liquid simulations] potential functions for proteins, energy minimizations for crystals of cyclic peptides and crambin. *J. Am. Chem. Soc.* **1988**, *110*, 1657-1666.

[32] Rivera-Fuentes, P.; Alonso-Gómez, J. L.; Petrovic, A.; Santoro, F.; Harada, N.; Berova, N.; Diederich F. Amplification of chirality in monodisperse, enantiopure alleno-acetylenic oligomers. *Angew. Chem. Int. Ed.* **2010**, *49*, 2247-2250.

[33] Clerc, J. T.; Sommerauer, H. A minicomputer program based on additivity rules for the estimation of 13c-nmr chemical shifts. *Anal. Chim. Acta* **1977**, *95*, 33-40.

[34] Pretsch, E.; Fürst, A. A computer program for the prediction of 13C-NMR chemical shifts of organic compounds. *Anal. Chim. Acta* **1990**, *229*, 17-25.

[35] Chen, L. R.; Robien, W. OPSI: A universal method for prediction of 13C-NMR spectra based on optimized additivity models. *Anal. Chem.* **1993**, *65*, 2282-2287.

[36] Bremser, W. HOSE, A novel structure code. *Anal. Chim. Acta* **1978**, *103*, 355-365.

[37] Meiler, J.; Meusinger, R.; Will, M. Fast determination of 13C NMR chemical shifts using artificial neural networks. *J. Chem. Inf. Comput. Sci.* **2000**, *40*, 1169-1176.

[38] Blinov, K. A.; Smurnyy, Y. D.; Elyashberg, M. E.; Churanova, T. S.; Kvasha, M.; Steinbeck, C.; Lefebvre, B. A.; Wiliams, A. J. Performance validation of neural network based C-13 NMR prediction using a publicly available data source. *J. Chem. Inf. Model* **2008**, *48*, 550-555.

[39] Altona, C. In *Vicinal Coupling Constants & Conformation of Biomolecules. Encyclopedia of NMR;* Grant, D. M., Morris, R., Eds.; Wiley: New York, **1996**; 4909-4923.

[40] Karplus, M. Vicinal proton coupling in nuclear magnetic resonance. *J. Am. Chem. Soc.* **1963**, *85*, 2870-2871.

[41] Haasnoot, C. A. G.; de Leeuw, F. A. A. M.; Altona, C. The relationship between proton-proton NMR coupling constants and substituent electronegativities-I. An empirical generalization of the karplus equation. *Tetrahedron* **1980**, *36*, 2783-2792.

[42] Navarro-Vázquez, A.; Carlos, J. C.; Sardina, F. J.; Casanueva, J.; Díez, E. A graphical tool for the prediction of vicinal proton-proton 3JHH coupling constants. *J. Chem. Inf. Comput. Sci.* **2004**, *44*, 1680-1685.

[43] Helgaker, T.; Jaszunski, M.; Ruud, K. Ab initio methods for the calculation of NMR shielding and indirect spin-spin coupling constants. *Chem. Rev.* **1999**, *99*, 293-352.

[44] Helgaker, T.; Jaszuński, M.; Pecul, M. The quantum-chemical calculation of NMR indirect spin-spin coupling constants. *Prog. Nucl. Magn. Reson. Spectrosc.* **2008**, *53*, 249-268.

[45] Bassarello, C.; Cimino, P.; Gomez-Paloma, L.; Riccio, R.; Bifulco, G. Recent acquisitions in the resolution of structural problems by NMR and quantum mechanical methods. *Recent Res. Dev. Org. Chem.* **2003**, *7*, 219-239.

[46] Bifulco, G.; Dambruoso, P.; Gomez-Paloma, L.; Riccio, R. Determination of relative configuration in organic compounds by NMR spectroscopy and computational methods. *Chem. Rev.* **2007**, *107*, 3744-3779.

[47] Bagno, A.; Saielli, G. Computational NMR spectroscopy: Reversing the information flow. *Theor. Chem. Accounts* **2007**, *117*, 603-619.

[48] Cheeseman, J. R.; Trucks, G. W.; Keith, T. A. Frisch, M. J. A comparison of models for calculating nuclear magnetic resonance shielding tensors. *J. Chem. Phys.* **1996**, *104*, 5497-5509.

[49] Wolinski, K.; Hinton, J. F.; Pulay, P. Efficient implementation of the gauge-independent atomic orbital method for NMR chemical shift calculations. *J. Am. Chem. Soc.* **1990**, *112*, 8251-8260.

[50] Ditchfield, R. Self-Consistent perturbation-theory of diamagnetism. gauge-invariant LCAO method for NMR chemical-shifts. *Mol. Phys.* **1974**, *27*, 789-807.

[51] Keith, T. A.; Bader, R. F. W. Calculation of magnetic response properties using a continuous set of gauge transformations. *Chem. Phys. Lett.* **1993**, *210*, 223-231.

[52] Wu, A.; Zhang, Y.; Xu, X.; Yan, Y. Systematic studies on the computation of nuclear magnetic resonance shielding constants and chemical shifts: the density functional models. *J. Comput. Chem.* **2007**, *28*, 2431-2442.

[53] Koch, W.; Holthausen, M. C. In *A Chemist's guide to Density Functional Theory;* Wiley-VCH Verlag GmbH & Co. KGaA: Weinheim, **2001**.

[54] Lee, A.; Handy, N.; Colwell, S. M. The density-functional calculation of nuclear shielding constants using london atomic orbitals. *J. Chem. Phys.* **1995**, *103*, 10095-10109.

[55] Wiitala, K. W.; Hoye, T. R.; Cramer, C. J. Hybrid density functional methods empirically optimized for the computation of 13C and 1H chemical shifts in chloroform solution. *J. Chem. Theory Comput.* **2006**, *2*, 1085-1092.

[56] Keal, T. W.; Tozer, D. J. The exchange-correlation potential in Kohn-Sham nuclear magnetic resonance shielding calculations. *J. Chem. Phys.* **2003**, *119*, 3015-3024.

[57] Allen, M. J.; Keal, T. W.; Tozer, D. J. Improved NMR chemical shifts in density functional theory. *Chem. Phys. Lett.* **2003**, *380*, 70-77.

[58] Zhang, Y.; Wu, A.; Xu, X.; Yan, Y. OPBE: A promising density functional for the calculation of nuclear shielding constants. *Chem. Phys. Lett.* **2006** *421*, 383-388.

[59] Zhao, Y.; Truhlar, D. G. Letter improved description of nuclear magnetic resonance chemical shielding constants using the M06-L Meta-Generalized-gradient-approximation density functional. *J. Phys. Chem. A* **2008**, *112*, 6794-6799.

[60] Van Voorhis, T.; Scuseria, G. E. A novel form for the exchange-correlation energy functional. *J. Chem. Phys.* **1998**, *109*, 400-410.

[61] Ramsey, N. Electron coupled interactions between nuclear spins in molecules. *Phys. Rev.* **1953**, *91*, 303-307.

[62] Manninen, P.; Vaara, J. Systematic gaussian basis-set limit using completeness-optimized primitive sets. A case for magnetic properties. *J. Comp. Chem.* **2006**, *27*, 434-445.

[63] Jensen, F. Basis set convergence of nuclear magnetic shielding constants calculated by density functional methods. *J. Chem. Theory Comput.* **2008**, *4*, 719-727.

[64] Jensen, F. The basis set convergence of spin-spin coupling constants calculated by density functional methods. *J. Chem. Theory Comput.* **2006**, *2*, 1360-1369.

[65] Deng, W.; Cheeseman, J.; Frisch, M. Calculation of nuclear spin-spin coupling constants of molecules with first and second row atoms in study of basis set dependence. *J. Chem. Theory Comput.* **2006**, *2*, 1028-1037.

[66] Zhao, Y.; Truhlar, D. Density functionals with broad applicability in chemistry. *Acc. Chem. Res.* **2008**, *41*, 157-167.

[67] Tomasi, J.; Mennucci, B.; Cammi, R. Quantum mechanical continuum solvation models. *Chem. Rev.* **2005**, *105*, 2999-3093.

[68] Dybiec, K.; Gryff-Keller, A. Remarks on GIAO-DFT predictions of 13 C chemical shifts. *Magn. Reson. Chem.* **2009**, *47*, 63-66.

[69] Tousek, J.; Van Miert, S.; Pieters, L. Van Baelen, G.; Hostyn, S.; Maes, B. U. W.; Lemiere, G. M.; Dommise, R.; Marek, R. Structural and solvent effects on the 13C and 15N NMR chemical shifts of indoloquinoline alkaloids: Experimental and DFT study. *Magn. Reson. Chem.* **2008**, *46*, 42-51.

[70] Bagno, A.; Rastrelli, F.; Saielli, G. Prediction of the 1H and 13C NMR spectra of [α]-d-Glucose in water by DFT methods and MD simulations. *J. Org. Chem.* **2007**, *72*, 7373-7381.

[71] Sarotti, A. M.; Pellegrinet, S. C. A Multi-standard approach for GIAO C-13 NMR calculations. *J. Org. Chem.* **2009**, *74*, 7254-7260.

[72] Braddock, D.; Rzepa, H. Structural reassignment of obtusallenes V, VI, and VII by GIAO-based density functional. *J. Nat. Prod.* **2008**, *71*, 728-730.

[73] Kaupp, M.; Malkina, O.; Malkin, V.; Pyykkö, P. How do spin-orbit-induced heavy-atom effects on NMR chemical shifts function? validation of a simple analogy to spin-spin coupling by density functional theory (DFT) calculations on some iodo compounds. *Chem. Eur. J.* **1998**, *4*, 118-126.

[74] Forsyth, D.; Sebag, A. Computed 13C NMR chemical shifts *via* empirically scaled GIAO shieldings. *J. Am. Chem. Soc.* **1997**, *119*, 9483-9494.

[75] Giesen, D.; Zumbulyadis, N. A hybrid quantum mechanical and empirical model for the prediction of isotropic C-13 shielding constants of organic molecules. *Phys. Chem. Chem. Phys.* **2002**, *4*, 5498-5507.

[76] Blanco, F.; Alkorta, I.; Elguero, J. Statistical analysis of 13C and 15N NMR chemical shifts from GIAO/B3LYP/6-311++ G** calculated absolute shieldings. *Magn. Reson. Chem.* **2007**, *45*, 797-800.

[77] Smith, S. G.; Goodman, J. M. Assigning the stereochemistry of pairs of diastereoisomers using GIAO NMR shift calculation. *J. Org. Chem.* **2009**, *74*, 4597-4607.

[78] Bagno, A.; Rastrelli, F.; Saielli, G. Toward the complete prediction of the 1H and 13C NMR spectra of complex organic molecules by DFT methods: application to natural substances. *Chem. Eur. J.* **2006**, *12*, 5514-5525.

[79] Schlegel, B.; Härtl, A.; Dahse, H. M.; Gollmick, F. A.; Gräfe, U.; Dörfelt, H.; Kappes, B. Hexacyclinol, a new antiproliferative metabolite of panus rudis HKI 0254. *J. Antibiot.* **2002**, *55*, 814-817.

[80] Clair, J. L. Total syntheses of hexacyclinol, 5-epi-hexacycyclinol, and desoxohexacyclinol unveil an antimalarial prodrug motif. *Angew. Chem. Int. Ed.* **2006**, *45*, 2769-2773.

[81] Rychnovsky, S. D. Predicting NMR spectra by computational methods: structure revision of hexacyclinol. *Org. Lett.* **2006**, *13*, 2895-2898.

[82] Porco Jr., J. A.; Su, S.; Lei, X.; Bardhan, S.; Rychnovsky, S. D. Total synthesis and structure assignment of (+)-hexacyclinol. *Angew. Chem. Int. Ed.* **2006**, *45*, 5790-5792.

[83] Saielli, G.; Bagno, A. Can two molecules have the same NMR spectrum? Hexacyclinol revisited. *Org. Lett.* **2009**, *11*, 1409-1412.

[84] Timmons, C.; Wipf, P. Density functional theory calculation of C-13 NMR shifts of diazaphenanthrene alkaloids: reinvestigation of the structure of samoquasine A. *J. Org. Chem.* **2008**, *73*, 9168-9170.

[85] Hu, G.; Liu, K.; Williams, L. J. The brosimum allene: a structural revision. *Org. Lett.* **2008**, *10*, 5493-5496.

[86] Xiao, W-L.; Lei, C.; Ren, J.: Liao, T-G.; Pu, J-X.; Pittman, Jr., C. U.; Lu, Y.; Zheng, Y-T.; Zhu, H-J.; Sun, H-D. Structure elucidation and theoretical investigation of key steps in the biogenetic pathway of schisanartane nortriterpenoids by using DFT methods. *Chem. Eur. J.* **2008**, *14*, 11584-11592.

[87] Chini, M. G.; Riccio, R.; Bifulco, G. DFT/NMR integrated approach: a valid support to the total synthesis of chiral molecules. *Magn. Reson. Chem.* **2008**, *46*, 962-968.

[88] Köck, M.; Grube, A.; Seiple, I. B.; Baran, P. S. The pursuit of Palau'amine. *Angew. Chem. Int. Ed.* **2007**, *46*, 6586-6594.

[89] Seiple, I. B.; Su, S.; Young, I. S.; Lewis, C. A.; Yamaguchi, J.; Baran, P. S. Total synthesis of Palau´amine. *Angew. Chem. Int. Ed.* **2010**, *49*, 1095-1098.

[90] Stappen, I.; Buchbauer, G.; Robien, W.; Wolschann, P. 13C-NMR spectra of santalol derivatives: a comparison of DFT-Based calculations and database-oriented prediction techniques. *Magn. Reson. Chem.* **2009**, *47*, 720-726.

[91] Sánchez-Pedregal, V. M.; Santamaría-Fernández, R.; Navarro-Vázquez, A. Residual dipolar couplings of freely rotating groups in small molecules. stereochemical assignment and side-chain conformation of 8-Phenylmenthol. *Org. Lett.* **2009**, *11*, 1471-1474.

[92] Subramaniam, G.; Karimi, S.; Phillips, D. Solution conformation of longifolene and its precursor by NMR and ab initio calculations. *Magn. Reson. Chem.* **2006**, *44*, 1118-1121.

[93] Muñoz, M. A.; Joseph-Nathan, P. DFT-GIAO 1H and 13C NMR prediction of chemical shifts for the configurational assignment of 6-hydroxyhyoscyamine diastereoisomers. *Magn. Reson. Chem.* **2009**, *47*, 578-584.

[94] Wiitala, K. W.; Cramer, C. J.; Hoye, T. R. Comparison of various density functional methods for distinguishing stereoisomers based on computed 1H or 13C NMR chemical shifts using diastereomeric penam β-lactams as a test set. *Magn. Reson. Chem.* **2007**, *45*, 819-829.

[95] Fattorusso, C.; Stendardo, E.; Appendino, G.; Fattorusso, E.; Luciano, P.; Romano, A.; Taglialatela-Scafati, O. Artarborol, a Nor-caryophyllane Sesquiterpene alcohol from artemisia arborescens. stereostructure assignment through concurrence of NMR data and computational analysis. *Org. Lett.* **2007**, *9*, 2377-2380.

[96] Schellman, J. A. Symmetry rules for optical rotation. *Acc. Chem. Res.* **1968**, *1*, 144-151.

[97] Polavarapu, P. L.; Petrovic, A.; Wang, F. Intrinsic rotation and molecular structure. *Chirality* **2003**, *15*, S143-S149.

[98] Polavarapu, P. L. Ab initio molecular optical rotations and absolute configurations. *Mol. Phys.* **1997**, *91*, 551-554.

[99] Polavarapu, P. L.; Zhao, C. A Comparison of ab initio optical rotations obtained with static and dynamic methods. *Chem. Phys. Lett*. **1998**, *296*, 105-110.

[100] Kondru, R. K.; Wipf, P.; Beratan, D. N. Theory-assisted determination of absolute stereochemistry for complex natural products *via* computation of molar rotation angles. *J. Am. Chem. Soc.* **1998**, *120*, 2204-2205.

[101] Giorgio, E.; Minichino, C.; Viglione, R. G.; Zanasi, R.; Rosini, C. Assignment of the molecular absolute configuration through the ab initio hartree-fock calculation of the optical rotation: can the circular dichroism data help in reducing basis set requirements? *J. Org. Chem.* **2003**, *68*, 5186-5192.

[102] Autschbach, J.; Patchkovskii, S.; Ziegler, T.; Van Gisbergen, S. J. A.; Baerends, E. J. Chiroptical properties from time-dependent density functional theory. II: optical rotations of small to medium sized organic molecules. *J. Chem. Phys.* **2002**, *117*, 581-592.

[103] Grimme, S. Calculation of frequency dependent optical rotation using density functional response theory. *Chem. Phys. Lett.* **2001**, *339*, 380-388.

[104] Krykunov, M.; Autschbach, J. Calculation of optical rotation with time-periodic magnetic-field-dependent basis functions in approximate time-dependent density-functional theory. *J. Chem. Phys.* **2005**, *123*, 114103.

[105] Stephens, P. J.; Devlin, F. J.; Cheeseman, J. R.; Frisch, M. J. Calculation of optical rotation using density functional theory. *J. Phys. Chem. A* **2001**, *105*, 5356-5371.

[106] Yabana, K.; Bertsch, G. F. Application of the time-dependent local density approximation to optical activity. *Phys. Rev. A* **1999**, *60*, 1271-1279.

[107] Pedersen, T. B.; Koch, H.; Boman, L.; Sánchez De Merás, A. M. J. Origin invariant calculation of optical rotation without recourse to london orbitals. *Chem. Phys. Lett*. **2004**, *393*, 319-326.

[108] Ruud, K.; Stephens, P. J.; Devlin, F. J.; Taylor, P. R.; Cheeseman, J. R.; Frisch, M. J. Coupled-cluster calculations of optical rotation. *Chem. Phys. Lett.* **2003**, *373*, 606-614.

[109] Tam, M. C.; Russ, N. J.; Crawford, T. D. Coupled cluster calculations of optical rotatory dispersion of (S)-Methyloxirane. *J. Chem. Phys.* **2004**, *121*, 3550-3557.

[110] Pecul, M.; Ruud, K.; Helgaker, T. Density functional theory calculation of electronic circular dichroism using london orbitals. *Chem. Phys. Lett.* **2004**, *388*, 110-119.

[111] Crassous, J.; Jiang, Z.; Schurig, V.; Polavarapu, P. L. Preparation of (+)-chlorofluoroiodomethane, determination of its enantiomeric excess and of its absolute configuration. *Tetrahedron Asymmetry* **2004**, *15*, 1995-2001.

[112] Crawford, T. D.; Owens, L. S.; Tam, M. C.; Schreiner, P. R.; Koch, H. Ab initio calculation of optical rotation in (P)-(+)-[4] Triangulane. *J. Am. Chem. Soc.* **2005**, *127*, 1368-1369.

[113] Polavarapu, P. L. The absolute configuration of bromochlorofluoromethane. *Angew. Chem. Int. Ed.* **2002**, *41*, 4544-4546.

[114] Rinderspacher, B. C.; Schreiner, P. R. Structure-property relationships of prototypical chiral compounds: case studies. *J. Phys. Chem. A* **2004**, *108*, 2867-2870.

[115] Specht, K. M.; Nam, J.; Ho, D. M. Determining absolute configuration in flexible molecules: a case study. *J. Am. Chem. Soc.* **2001**, *123*, 8961-8966.

[116] Olsen, J.; Jørgensen, P. Time-dependent response theory with applications to self-consistent field and multiconfigurational self-consistent field wave functions. *Modern Electron. Struct. Theory* **1995**, *2*, 857-990.

[117] Giorgio, E.; Viglione, R. G.; Zanasi, R.; Rosini, C. Ab Initio calculation of optical rotatory dispersion (ORD) curves: a simple and reliable approach to the assignment of the molecular absolute configuration. *J. Am. Chem. Soc.* **2004**, *126*, 12968-12976.

[118] Bauernschmitt, R.; Ahlrichs, R. Treatment of electronic excitations within the adiabatic approximation of time dependent density functional theory. *Chem. Phys. Lett.* **1996**, *256*, 454-464.

[119] Furche, F.; Ahlrichs, R. Absolute configuration of D2-Symmetric fullerene C84. *J. Am. Chem. Soc.* **2002**, *124*, 3804-3805.

[120] Lackowski, K. Z.; Baranowska, A. Conformational analysis and optical rotation of carene β-Amino alcohols: A DFT study. *Eur. J. Org. Chem.* **2009**, 4600-4605.

[121] Kwit, M.; Rozwadowska, M. D.; Gawroński, J.; Grajewska, A. Density Functional theory calculations of the optical rotation and electronic circular dichroism: the absolute configuration of the highly flexible trans-isocytoxazone revised. *J. Org. Chem.* **2009**, *74*, 8051-8063.

[122] Becke, A. D. Density-functional exchange-energy approximation with correct asymptotic behavior. *Phys. Rev. A* **1988**, *38*, 3098-3100.

[123] Lee, C.; Yang, W.; Parr, R. G. Development of the Colle-Salvetti correlation-energy formula into a functional of the electron density. *Phys. Rev. B* **1988**, *37*, 785-789.

[124] Cheeseman, J. R.; Frisch, M. J.; Devlin, F. J.; Stephens, P. J. Hartree-Fock and density functional theory ab initio calculation of optical rotation using giaos: basis set dependence. *J. Phys. Chem. A* **2000**, *104*, 1039-1046.

[125] Stephens, P. J.; Devlin, F. J.; Cheeseman, J. R.; Frisch, M. J.; Mennucci, B.; Tomasi, J. Prediction of optical rotation using density functional theory: 6,8-Dioxabicyclo[3.2.1]octanes. *Tetrahedron Asymmetry* **2000**, *11*, 2443-2448.

[126] Mennucci, B.; Tomasi, J.; Cammi, R. Polarizable continuum model (PCM) calculations of solvent effects on optical rotations of chiral molecules. *J. Phys. Chem.* **2002**, *106*, 6102-6113.

[127] Stephens, P. J.; McCann, D. M.; Cheeseman, J. R.; Frisch, M. J. Determination of Absolute Configurations Of Chiral Molecules Using Ab Initio Time-Dependent Density Functional Theory Calculations Of Optical Rotation: How Reliable Are Absolute Configurations Obtained For Molecules With Small Rotations? *Chirality* **2005**, *17*, S52-S64.

[128] London, F. Théorie quantique des courants interatomiques dans les combinaisons aromatiques. *J. Phys. Radium* **1937**, *8*, 397-409.

[129] Clark, T.; Chandrasekhar, J.; Spitznagel, G. W.; Schleyer, P. V. R. Efficient diffuse function-augmented basis sets for anion calculations. III. The 3-21+G basis set for first-row elements, Li-F. *J. Comput. Chem.* **1983**, *4*, 294-301.

[130] Frisch, M. J.; Pople, J. A.; Binkley, J. S. Self-Consistent molecular orbital methods 25. supplementary functions for gaussian basis sets. *J. Chem. Phys.* **1984**, *80*, 3265-3269.

[131] Gill, P. M. W.; Johnson, B. G.; Pople, J. A.; Frisch, M. J. The performance of the Becke-Lee-Yang-Parr (B-LYP) density functional theory with various basis sets. *Chem. Phys. Lett.* **1992**, *197*, 499-505.

[132] Krishnan, R.; Binkley, J. S.; Seeger, R.; Pople, J. A. Self-consistent molecular orbital methods. XX. a basis set for correlated wave functions. *J. Chem. Phys.* **1980**, *72*, 650-654.

[133] McLean, A. D.; Chandler, G. S. Contracted gaussian basis sets for molecular calculations. I. second row atoms, Z=11-18. *J. Chem. Phys.* **1980**, *72*, 5639-5648.

[134] Crawford, T. D.; Stephens, P. J. Comparison of time-dependent density-functional theory and coupled cluster theory for the calculation of the optical rotations of chiral molecules. *J. Phys. Chem. A* **2008**, *112*, 1339-1345.

[135] Elguero, J.; Marzin, C.; Katritzky, A. R.; Linda, P. The Tautomerism of Heterocycles. *Adv. Heterocycl. Chem.* **1976**, Suppl. 1.

[136] Jia, L.; Shafirovich, V.; Shapiro, R.; Geacintov, N. E.; Broyde, S. Spiroiminodihydantoin lesions derived from guanine oxidation: structures, energetics, and functional implications. *Biochemistry (N. Y.)* **2005**, *44*, 6043-6051.

[137] Durandin, A.; Jia, L.; Crean, C. Assignment of absolute configurations of the enantiomeric spiroiminodihydantoin nucleobases by experimental and computational optical rotatory dispersion methods. *Chem. Res. Toxicol.* **2006**, *19*, 908-913.

[138] Ding, S.; Jia, L.; Durandin, A. Absolute configurations of spiroiminodihydantoin and allantoin stereoisomers: comparison of computed and measured electronic circular dichroism spectra. *Chem. Res. Toxicol.* **2009**, *22*, 1189-1193.

[139] Giorgio, E.; Roje, M.; Tanaka, K. Determination of the absolute configuration of flexible molecules by ab initio ord calculations: a case study with cytoxazones and isocytoxazones. *J. Org. Chem.* **2005**, *70*, 6557-6563.

[140] Harada, N.; Nakanishi, K. Circular Dichroic Spectroscopy – Exciton Coupling in Organic Chemistry. University Science Books, Mill Valley, CA **1983**.

[141] Stephens, P. J.; Harada, N. ECD Cotton Effect Approximated by the Gaussian Curve and Other Methods *Chirality* **2010**, *22*, 229-233.

[142] Bodensieck, A.; Fabian, W. M. F.; Kunert, O.; Belaj, F.; Jahangir, S.; Schühly, W.; Bauer, R. Absolute configuration of eremophilane sesquiterpenes from Petasites hybridus: Comparison of experimental and calculated circular dichroism spectra. *Chirality* **2009**, *22*, 308-319.

[143] Grimme, S.; Waletzke, M. A combination of Kohn-Sham density functional theory and multi-reference configuration interaction methods. *J. Chem. Phys.* **1999**, *111*, 5645-5655.

[144] Stephens, P. J.; Pan, J.-J.; Devlin, F. J.; Urbanová, M.; Julínek, O.; Hájíček, J. Determination of the absolute configurations of natural products *via* density functional theory calculations of vibrational circular dichroism, electronic circular dichroism, and optical rotation: the iso-schizozygane alkaloids isoschizogaline and isoschizogamine. *Chirality* **2008**, *20*, 454-470.

[145] Alonso-Gómez, J. L.; Petrovic, A. G.; Harada, N.; Rivera-Fuentes, P.; Berova, N.; Diederich, F. Chiral induction from allenes into twisted l,l,4,4-tetracyanobuta-1,3- dienes (TCBDs): Conformational assignment by circular dichroism spectroscopy. *Chem. Eur. J.* **2009**, *15*, 8396-8400.

[146] Nafie, L. A. Dual polarization modulation: a real-time, spectral-multiplex separation of circular dichroism from linear birefringence spectral intensities. *Appl. Spectrosc.* **2000**, *54*, 1634-1645.

[147] Nafie, L. A.; Buijs, H.; Rilling, A.; Cao, X.; Dukor, R. K. Dual source Fourier transform polarization modulation spectroscopy: an improved method for the measurement of circular and linear dichroism. *Appl. Spectrosc.* **2004**, *58*, 647-654.

[148] Guo, C.; Shah, R. D.; Dukor, R. K.; Freedman, T. B.; Cao, X.; Nafie, L. A. Fourier transform vibrational circular dichroism from 800 to 10,000 cm-1: Near-IR-VCD spectral standards for terpenes and related molecules. *Vib. Spectrosc.* **2006**, *42*, 254-272.

[149] Stephens, P. J. Theory of vibrational circular dichroism. *J. Phys. Chem.* **1985**, *89*, 748-752.

[150] Stephens, P. J. Gauge dependence of vibrational magnetic dipole transition moments and rotational strengths. *J. Phys. Chem.* **1987**, *91*, 1712-1715.

[151] Buckingham, A. D.; Fowler, P. W.; Galwas, P. A. Velocity-Dependent property surfaces and the theory of vibrational circular dichroism. *Chem. Phys.* **1987**, *112*, 1-14.

[152] Urbanova, M. Bioinspired interactions studied by vibrational circular dichoism. *Chirality* **2009**, *21*, e215-e230.

[153] Stephens, P. J.; Devlin, F. J.; Pan, J. The determination of the absolute configurations of chiral molecules using vibrational circular dichroism (VCD) spectroscopy. *Chirality* **2008**, *20*, 643-663.

[154] Nafie, L. A. Vibrational Circular Dichroism: A new tool for the solution-state determination of the structure and absolute configuration of chiral natural product molecules. *Nat. Prod. Commun.* **2008**, *3*, 451-166.

[155] Taniguchi, T.; Miura, N.; Nishimura, S.; Monde, K. Vibrational circular dichroism: chiroptical analysis of biomolecules. *Mol. Nutr. Food Res.* **2004**, *48*, 246-254.

[156] Freedman, T. B.; Cao, X.; Dukor, R.; Nafie, L. A. Absolute configuration determination of chiral molecules in the solution state using vibrational circular dichroism. *Chirality* **2003**, *15*, 743-758.

[157] Minick, D. J.; Copley, R. C. B.; Szewczyk, J. R.; Rutkowske, R. D.; Miller, L. A. An investigation of the absolute configuration of the potent histamine H3 receptor antagonist GT-2331 using vibrational circular dichroism. *Chirality* **2007**, *19*, 731-740.

[158] Yang, G.; Xu, Y. The effects of self-aggregation on the vibrational circular dichroism and optical rotation measurements of glycidol. *Phys. Chem. Chem. Phys.* **2008**, *10*, 6787-6795.

[159] Cichewicz, R. H.; Clifford, L. J.; Lassen, P. R. Stereochemical determination and bioactivity assessment of (S)-(+)-curcuphenol dimers isolated from the marine sponge didiscus aceratus and synthesized through laccase biocatalysis. *Bioorg. Med. Chem. Lett.* **2005**, *13*, 5600-5612.

[160] Cerda-García-Rojas, C. M.; Catalán, C. A. N.; Muro, A. C.; Joseph-Nathan, P. Vibrational circular dichroism of africanane and lippifoliane sesquiterpenes from lippia integrifolia. *J. Nat. Prod.* **2008**, *71*, 967-971.

[161] Cerda-García-Rojas, C. M.; García-Gutiérrez, H. A.; Hernández-Hernández, J. D.; Román-Marín, L. U.; Joseph-Nathan, P. Absolute configuration of verticillane diterpenoids by vibrational circular dichroism. *J. Nat. Prod.* **2007**, *70*, 1167-1172.

[162] Lassen, P. R.; Skytte, D. M.; Hemmingsen, L. Structure and absolute configuration of nyasol and hinokiresinol *via* synthesis and vibrational circular dichroism spectroscopy. *J. Nat. Prod.* **2005**, *68*, 1603-1609.

Received: 05 January, 2010 Revised: 11 February, 2010 Accepted: 11 February, 2010